THE CRYSTAL STRUCTURE OF BONITO HEART FERROCYTOCHROME C

—— OXIDATION OF THE PROTEIN IN CRYSTALLINE STATE

TOMITAKE TSUKIHARA

The Crystal Structure of Bonito Heart Ferrocytochrome *c*

—— Oxidation of the Protein in Crystalline State

A Doctoral Thesis

Submitted by

Tomitake Tsukihara

to

Faculty of Science

Osaka University

1973

ACKNOWLEDGEMENTS

This work was performed at the Kakudo Laboratory, Institute for Protein Research, Osaka University. I am greatly indebted to Professor Masao Kakudo for his cordial guidances and constant encouragements. I am grateful to Dr. Tamaichi Ashida for his kind guidances and encouragements. I wish to express the appreciation to Dr. Nobuo Tanaka for his fruitful discussions. My thanks are due to Mr. Takashi Yamane for his valuable help throughout this work, and to Miss. Sachiko Bando and Kenichi Sakaguchi for their kind assistance in experiments.

I am also grateful to Professor Yukiteru Katsube of Tottori University for his constant encouragements. I wish to express my gratitude to Drs. Tsunehiro Takano of Medical Research Council Laboratory of Molecular Biology, Cambridge, Tatzuo Ueki of Faculty of Engineering Science, Osaka University and Akio Sugihara for their advices.

CONTENTS

I. Introduction---------- 1

I-1 History of cytochromes---------- 1

I-2 Chemical and physical properties of cytochrome c--- 1

I-3 Physiological function of cytochrome c---------- 3

II. Crystal structure analysis of bonito heart ferrocytochrome c----------11

II-1 Experimental----------11

Purification and crystallization of the protein--11

Modified flow cell----------11

Preparation of isomorphous heavy atom derivatives----------12

Data collection----------13

II-2 Phase determination----------14

Location of heavy atoms and refinement of their parameters----------14

Calculation of electron density map----------15

II-3 Main chain folding, heme and some residues--------16

III. Structural change of cytochrome c upon oxidation of heme iron in crystalline state----------31

III-1 Experimental----------31

Oxidation of the crystals----------31

Data collection----------32

III-2 Change of observed structure amplitude by oxidation of the crystal----------32

III-3 Theory of difference Fourier synthesis----------33

III-4 Difference electron density between the oxidized and the reduced crystals---------- 34

IV. Discussion----------41
IV-1 Oxidation-reduction mechanism of cytochrome c-----41
Cyclic oxidation-reduction----------41
Pathway of an electron at reduction----------44
Degradation of the oxidase activity upon chemical modifications and a possible oxidation mechanism of the protein----------49
IV-2 Anion catching and it's physiological meanings----50
Anion catching scheme and oxidation mechanism of the protein----------50
Mitochondrial anion transport of the protein-----53
Oxidative phosphorylation----------53
References----------66
List of publications----------70

I. Introduction

I-1 History of cytochromes

As early as 1886, MacMunn observed the spectral absorption bands of the cytochromes in large variety of organisms and tissues.[1] But these MacMunn's discoveries had been ignored until Keilin rediscovered the four-band spectrum[2], and confirmed MucMunn's spectroscopic observations. Keilin showed that these proteins were repeatedly oxidized and reduced during cellular respiration, and that the sequence of electron transfer to oxygen is as follows,

$$\text{substrate} \longrightarrow \text{dehydrogenase} \longrightarrow \text{cytochromes} \longrightarrow \text{cytochrome oxidase} \longrightarrow O_2 \ .$$

Biological and chemical studies about cytochromes have been started by the Keilin's rediscovery.

About 250 species of cytochromes have been discovered. Cytochrome c is most precisely investigated in all the types of cytochromes. In 1961, amino acid sequence was fully established for horse heart cytochrome c by two groups[3,4] Since then the primary structures of cytochrome c have been determined for about 40 species[5]. The serial studies of the primary structure of the protein have pioneered comparative biochemistry at molecular level. The study of tertiary structure coupled with chemical modification and spectroscopic studies is revealing the oxidation-reduction mechanism of the protein.

I-2 Chemical and physical properties of cytochrome c

Proteins containing heme c (Fig.1) with absorption bands

of α, β, and γ are named cytochrome C. Cytochrome C's of animals, yeast and others, with α-band at 550mμ are named cytochrome c. The protein has an isoelectric point of pH 10. and their molecular weights are about 12,500.

All the proteins from vertebrate species are 104 or 103 residues long, and lack a free α-amino group at amino terminal residue, the chain invariably starting with N-acetylglycine. To contrast with this situation, the proteins from every non-vertebrate species so far examined have peptide chains longer than 104 residues and carry, in place of acetyl group, several extra amino acids, the terminal α-amino group being free. In Fig.3 amino acid sequences are shown for 38 species of cytochrome c[5]. It can be seen in the sequences the residues of 32 positions being completely invariant, and other 22 positions remaining phylogenetic constancy of structure expressed in so-called "conservative" substitution. This substitution occurs in the residues which are considered mutually interchangeable, in the sense that their chemical structures are similar to the extent that they are capable of the same structural role. The residues in above 54 positions could be considered particularly important for the appearance of physiological functions.

Many authors have observed conformational differences of the protein brought about by oxidation or reduction of heme iron. Zeile and Reuter showed that the oxidized protein was adsorbed more readily on kaolin than the reduced[8]. Jonxis found a difference in the surface tension of monomolecular layer of the protein between the two oxidation

states[9]. The spectroscopic tyrosyl ionization curves of the two oxidation states indicated for the reduced protein to have greater structural rigidity.[10] Chemical reactivity of the protein moiety itself is also quite different. Digestion of polypeptide chain by proteolytic enzymes is slower with the reduced than it is with the oxidized.[11] Other differences in the physico-chemical properties between the two oxidation states have been detected by nuclear magnetic resonance,[12] Mössbauer effect,[13] CD spectra[14,15] and ORD spectra.[16] The differences of physico-chemical and biological properties are summarized in Table 1.

I-3 Physiological function of cytochrome c

Cytochrome c is an electron carrier in the oxidation-reduction system of respiratory chain in the cell mitochondria. The protein oxidizes cytochrome c_1, and reduces oxygen molecule in co-operation with cytochrome a.[22] The electron transport is coupled with phosphorylation of ADP(oxidative phosphorylation). The oxidative phosphorylation and the sequence of electron transfer are shown in Fig.5. It is one of the purposes of present study to show the mechanism of electron transfer by the protein.

Recently, another possible physiological function was proposed by Margoliash et al.[21] It was suggested by similarity between ion binding properties of cytochrome c and permeability properties of mitochondrial membrane that the protein may be an ion transport carrier of the inner mitochondrial membrane. The other purposes of the present work are to

indicate ion binding scheme of the oxidized protein and the reduced, and it's physiological meanings.

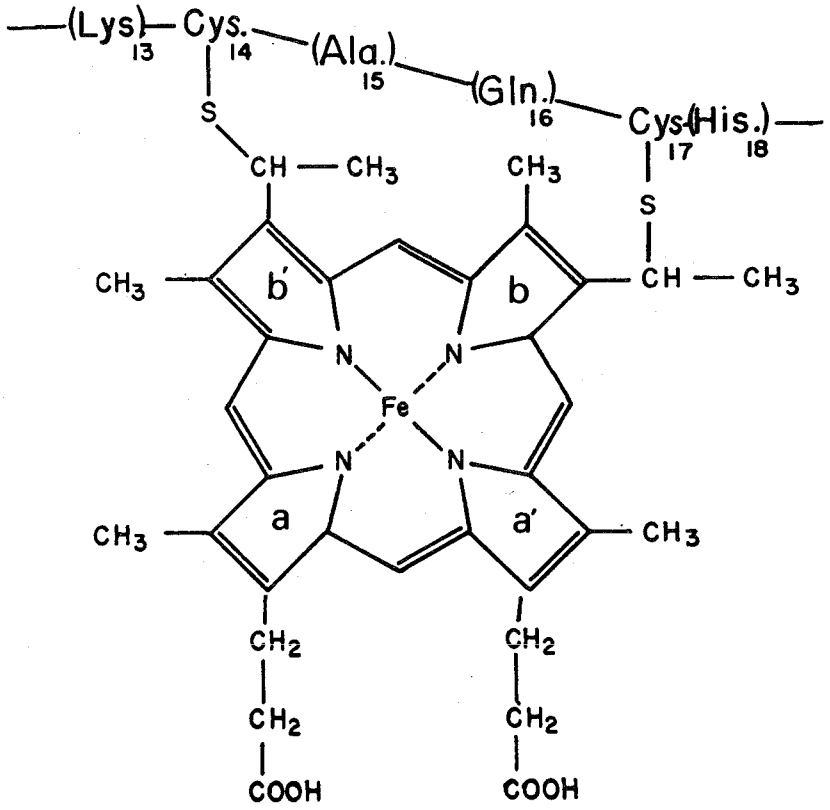

Fig. 1. Chemical structure of heme c. The heme is covalently linked to the protein through two thioether bonds to the two cysteinyl residues in the invariable sequence, —Cys—X—Y—Cys—His—, which is formed by the residues 14 through 18. In this paper four pyrrole rings are named "a", "b", "a'", and "b'" for convenience sake, respectively.

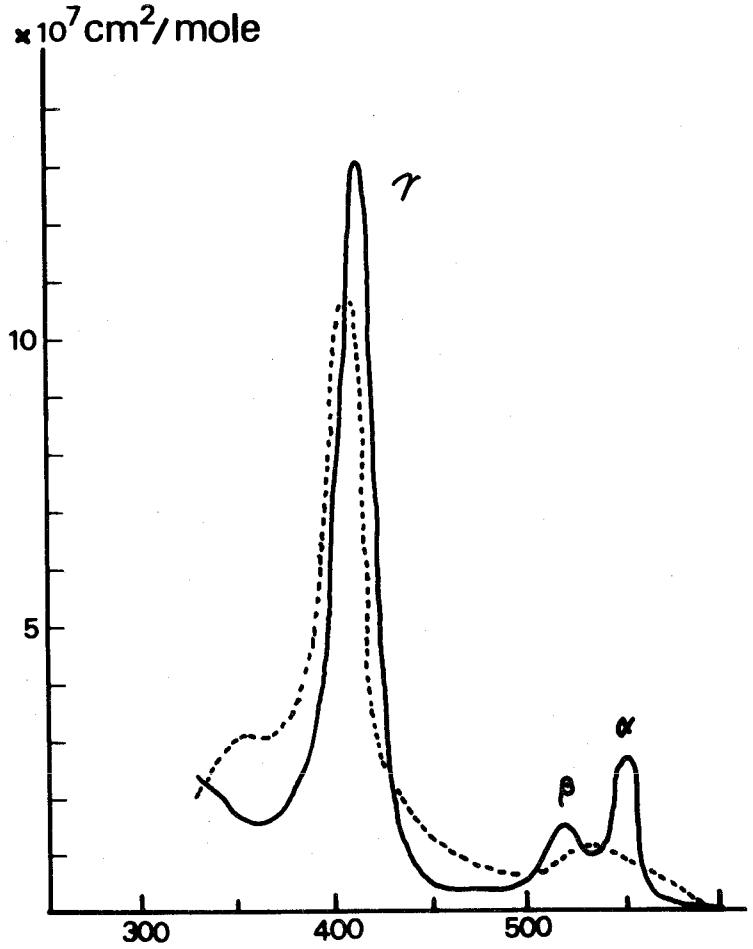

Fig. 2 Absorption spectra of oxidized (dotted line) and reduced (full line) cytochrome c's from horse heart; this preparation contained 0.45% iron.[6] The specific α-band of the reduced protein disappears in the spectrum of the oxidized one. Molar absorption coefficient of γ-band is about 28 $mM^{-1}cm^{-1}$.

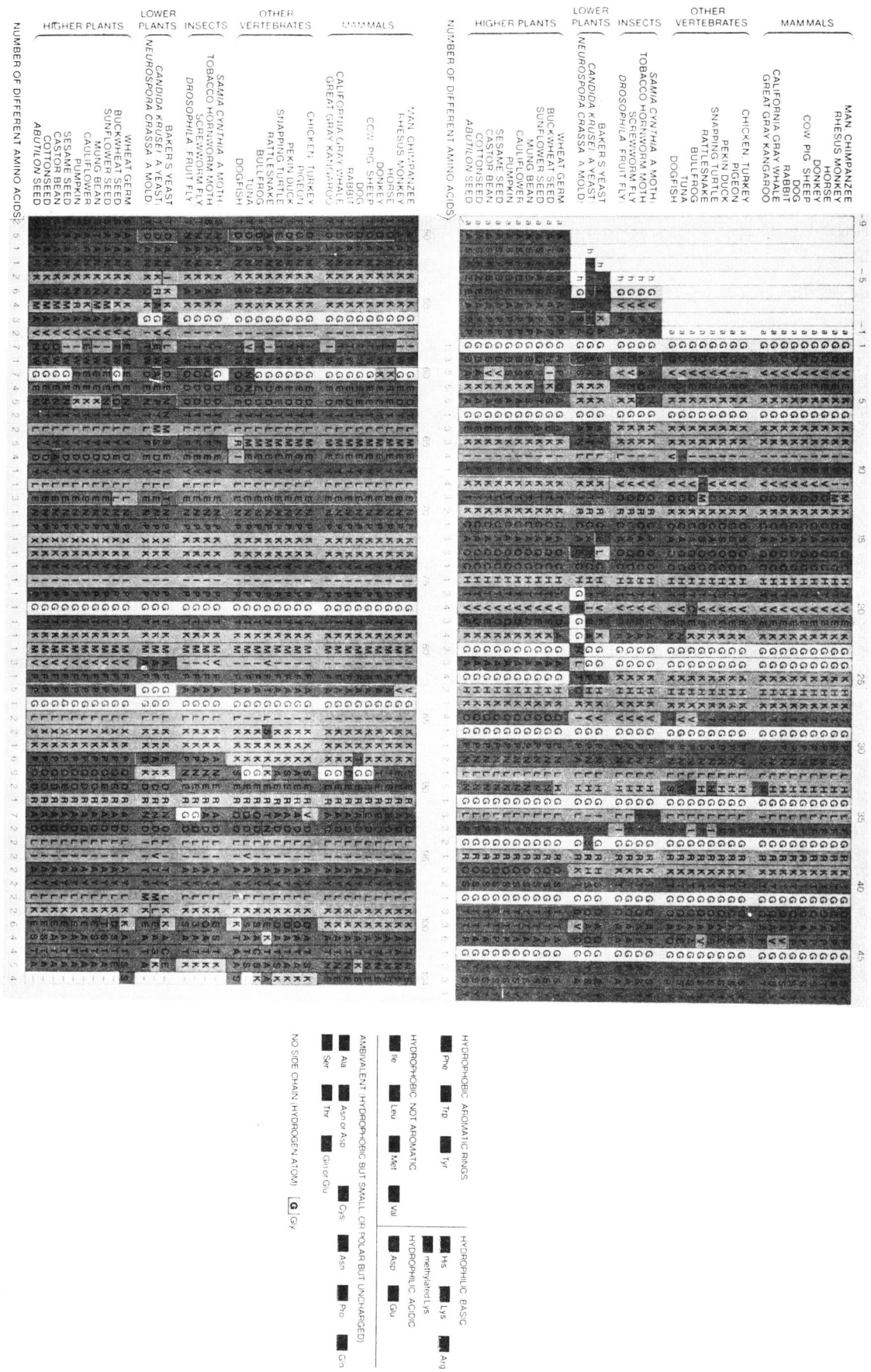

Fig. 3. Amino acid sequences of 38 species of cytochrome c.[5)]

CH_3-CO-NH-GLY-Asp-Val-Ala-LYS-GLY-LYS-LYS-Thr-Phe-Val- 11

-Gln-LYS-Cys-Ala-Gln-Cys-His-Thr-Val-Glu-Asn-GLY-GLY- 24

-LYS-His-LYS-Val-GLY-Pro-Asn-Leu-Trp-GLY-Leu-Phe-GLY- 37

-Arg-LYS-Thr-GLY-Gln-Ala-Glu-GLY-Tyr-Ser-Tyr-Thr-Asp- 50

-Ala-Asn-LYS-Ser-LYS-GLY-Ilu-Val-Trp-Asn-Glu-Asn-Thr- 63

-Leu-Met-Glu-Tyr-Leu-Glu-Asn-Pro-LYS-LYS-Tyr-Ilu-Pro- 76

-GLY-Thr-LYS-Met-Ilu-Phe-Ala-GLY-Ilu-LYS-LYS-LYS-Gly- 89

-Glu-Arg-Gln-Asp-Leu-Val-Ala-Tyr-Leu-LYS-Ser-Ala-Thr- 102

-Ser-COOH

Fig. 4. Amino acid sequence of bonito heart cytochrome c.[7] The underlined residues expressed with capital letters are glycines and lysines which are evolutionally conservative. The molecule lacks a free α-amino group at the amino terminal residue, the chain starting with N-acetylglycine as detected in all other vertebrate cytochrome c. The protein as that of tuna fish is 103 residues long, lacking one of the lysyl residues in position 99-100. The cytochrome c is basic, and contains a preponderance of lysyl residues. These residues tend to occur in distinct cluster along the protein chain. Glycyl residues are also contained in cytochrome c more than other species of proteins. Most of these lysyl and glycyl residues are evolutionally invariable.

Table 1. Difference of properties between two oxidation states

	oxidized	reduced
adsorption by kaolin	readily	less readily[8]
viscosity in 10% saturated ammonium salfate solution	high	low
surface tension of monolayer	high	low[9]
pKa of Tyr	12.1	12.6[10]
digestion by proteinase	readily	slowly[11]
carboxy-methylation of Met(80)	possible	impossible[17]
cyanogenation	possible in physiological condition	possible only at high temp. and high pH[18]
Cotton effect arising from γ-band	positive	negative[14,15]
hydrogen-deuterium exchange of peptide hydrogens within 5 minutes	68%	59%[19]
dessociation of cyan from cyano-cytochrome c	ΔH=15 Kcal/mole ΔS=-30 eu.	21.4 Kcal/mole[20] 2.1 eu.
contribution to coordination bonds of 4s electrons in iron	10%	35%[13]
absorption spectra	γ-band	γ-, α-, β-bands
ion binding ; Cl^-	one more than reduced form	[21]
; Ca^{2+}		one more than oxidized one

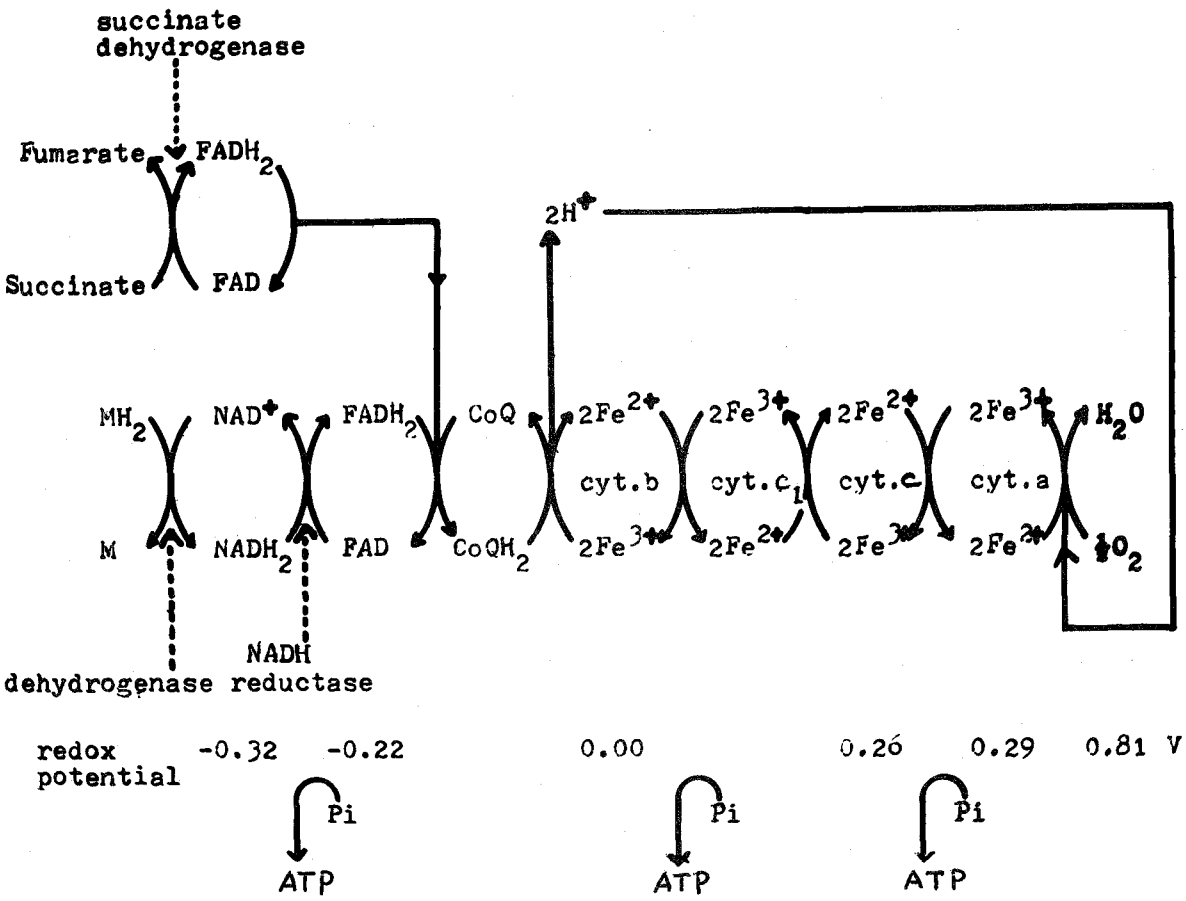

Fig. 5. Hydrogen and electron transport systems and oxidative phosphorylation in cellular respiration. An electron is transferred from a substrate exhibiting low redox potential to oxygen having higher redox potential through flavoproteins, cytochromes and other substances. The electron transport is coupled with ATP synthesis at three sites of the respiratory chain. The ATP is a high energy compound in the mitochondria.

II. Crystal structure analysis of bonito ferrocytochrome c

II-1 Experimental

Purification and crystallization of the protein

The protein was extracted from bonito hearts by the method of Margoliash and Walasek.[23] Desalting was carried out by the use of a Sephadex G-25 column, instead of dialysis. The main steps of purification and extraction are shown in Table 2. At the final step of the purification the protein charged to Amberlite IRC-50 was eluted with 10% saturated ammonium sulfate solution(10% AS, pH 8.0). The crystallization process of bonito ferrocytochrome c was observed by use of photographs, and is shown in Fig.6. At the begining of the crystallization, amorphous turbidity appeared and red color of the solution gradually disappeared. This phenomenon shows that the protein is diluted in the solution and concentrated in the amorphous. After one or two days very small crystals were found among the amorphous. These crystals eat the amorphous and gradually grow. If we give a shock to a test tube containing the protein solution, the amorphous substances are precipitated and crystal growth stops. The precipitation may disturb the crystal growth.

In order to get suitable crystals for the structure analysis it is a key point that the extraction and purification should be done quickly at most within two weeks, and the crystallization should be undertaken carefully.

Modified flow cell

A modified flow cell is devised for the determination of soaking condition of heavy atoms. The new version of the flow cell is schematically shown in Fig.7. A equatorial type of the aluminium arm was designed in order to lower the height of a crystal to the position of the incident x-ray beam. The polyethylene tube between the arms in earlier version by Wyckoff et al.[24] was replaced by a thin wall (10μ) quartz capillary. A crystal was fixed by Sephadex chunks(G-25 coarse), and the chunks were folded by cotton linter. This unit has the advantages of the eliminating the diffraction pattern of polyethylene crystal and lowering background as shown in Fig.8.

The structural change of the crystal caused by soaking solution was investigated by this modified flow cell. The solutions were continuously flowed in the capillary, and at the same time intensities and profiles of several reflections were observed. The changes of the intensities and profiles were not caused by the solution in the pH region between 5.0 and 8.0, so that all the preparations of heavy atom derivatives were undertaken in this pH region. Drastic change of the diffraction pattern was observed in the case where the solution of $K_3UO_2F_5$(pH 6.2) was flowed 10 ml per day. The change was accomplished and the mosaicity of the crystal was not increased within 2 or 3 days.

Preparation of isomorphous heavy atom derivatives

All the heavy atom derivatives were prepared by soaking method. The chemical modification method was not applied

successfully. The soaking condition for each heavy atom derivative is listed in Table 4. The soaking solution were adjusted to pH 6.0 with phosphate buffer except that of potassium uranyl fluoride, $K_3UO_2F_5$. In this case, since a precipitate is formed by phosphate, the buffer was excluded from the solution which was adjusted to pH 6.2 by concentrated aquous ammonia. These derivatives have approximately the same crystal lattice as the native. The heavy atom sites of all the derivatives are assigned, but only three derivatives were finally used for the calculation of phase angles for the reasons described in the following section.

Data collection

The crystal is orthorhombic, space group being $P2_12_12_1$ with eight molecules in the unit cell of dimensions: $\underline{a}$=57.54, $\underline{b}$=84.71, and $\underline{c}$=37.74Å. Intensity data were collected by a computer-controled four-circle diffractometer with target-to-crystal distance of 28 cm and crystal-to-counter distance of 20 cm. All the measurements were undertaken with moving-crystal stationary-counter method (ω-scan), by using nickel filtered Cu-Kα radiation. The moving-crystal moving-counter method was not employed, because the method can not avoid decrease of observed intensity of reflections from same heavy atom derivatives whose mosaicity increase than the native crystal. In all the cases of the measurements, crystals of approximate dimensions, 0.1x0.7x0.7mm^3 were mounted with the c-axis parallel to the ϕ-axis of the diffractometer. Absorption corrections were carried out by Furnas' method.[25)]

During the measurements, three monitored reflections of (0 4 2), (4 20 5), and (0 15 6) were inserted every fifty reflections. When the intensity change of these reflections effected by the oxidation of the crystal or the intensity decrease by x-ray damage of the crystal were observed, the measurement was terminated.

The averaged differences of structure amplitude among three sets of the data of reduced crystals are below 2 or 3% in F, and that between a reduced crystal and 50% oxidized crystals is about 6%.

II-2 Phase determination

Location of heavy atoms and refinement of their parameters

The difference Patterson function calculated with the coefficient of $(|Fph|-|Fp|)^2$ and the difference Fourier syntheses with $(|Fph|-|Fp|)\exp(i\phi p)$ showed heavy atom sites. Where Fph is the structure factor of a heavy atom derivative, Fp and ϕp are the structure factor and the phase angle of the native crystal, respectively. The parameters of heavy atoms were refined by the least-squares calculations minimizing the sum$_i$ of

$$m(|Fph|_{obs}-k|Fp_{obs}+Fh_{calc}|\ \exp(-\Delta B(\sin\theta/\lambda)^2))^2,$$

where

$$Fh_{calc}=\sum_j G_j \bar{f} \exp(2\pi i(hx_j+ky_j+lz_j))\exp(-B_j(\sin\theta/\lambda)^2),$$

m : figure of merit defined as following section,

$\bar{f}$: unitary structure factor,

G_j: occupancy of heavy atom in electron.

The final parameters for these derivatives are listed in

Table 5. The derivative of $HgI_4^=$ was not used for the phase determination, because the reagent deteriorated the crystal structure. The derivative of $PtCl_4^=$ was used only in the early stage of the calculation because of low isomorphism.

In the crystal $HgI_4^=$ ion is located closely at the sulfur atom of Cys(17), which links the heme group to the polypeptide chain. This ion binding may initiate the hydrolysis of the thioether bond by mercurial salts.[26] The mechanism of the hydrolysis seems to be reasonable, because the other sulfur atom of thioether bond is buried in the protein. The ion of $PtCl_4^=$ is located closely at Met(65) as in the case of horse ferricytochrome c. The $UO_2F_5^=$ ion is surrounded by lysyl groups of Lys 13, 86, 87 and 88.

Calculation of electron density map

The phase angles and the figure of merit of the native crystal were determined according to the following equations,[27,28]

$$m \cos(\phi p) = \int_0^{2\pi} P(\phi) \cos(\phi)\, d\phi \,/\, \int_0^{2\pi} P(\phi)\, d\phi,$$

$$m \sin(\phi p) = \int_0^{2\pi} P(\phi) \sin(\phi)\, d\phi \,/\, \int_0^{2\pi} P(\phi)\, d\phi,$$

where

$$P(\phi) = \exp\left(-\sum \varepsilon_j^2(\phi) \,/\, 2E_j^2 \right),$$

ε_j : lack of closure ,

$$E_j^2 = \langle |Fph_j - Fp - Fh_j|^2 \rangle ,$$

these relation are shown in Fig.8, and E_j was determined by use of all the reflections.

The electron density of the native crystal was calculated

at 2.3 Å resolution with the coefficient of $m|Fp|\exp(i\phi p)$.[27,28] No modification to minimize termination of series errors was not applied. The map calculated with four derivatives including $PtCl_4^=$ derivative seemed to give some unreasonable features in the vicinity of Pt-position. Therefore the derivative was not used for the final calculation of the electron density map at 2.3Å resolution.

The root mean squares of error in electron density, $\sigma(\rho)$, estimated by the following equation,[27,28]

$$\sigma^2(\rho)=2\sum|Fp|^2(1-m^2)/V^2$$

was 0.075e/Å^3, where V is the volume of the unit cell of the crystal. An averaged figure of merit was 0.67.

II-3 Main chain folding, heme and some residues

The highest peak of the electron density of 2.3e/Å^3 indicates the iron atom of the heme. The electron density map of successive section including the peak is shown in Fig.11. The fifth and sixth ligands of the heme iron are clearly visible. These are the same residues of His(18) and Met(80) as those of the horse oxidized protein.[29] All the four pyrrole rings are also revealed in the electron density map as stereoscopically shown in Fig.12. One of the propionic groups of the heme is buried in the molecule and bound to the indole group of Trp(59) through a N-H---O hydrogen bond (Fig.13). All the 103 residues were assigned in the map. At the present stage the positional parameters of the residues have not been refined yet.

The amino-terminal ten residues and the carboxyl-

terminal fourteen residues construct α-helices. Whole structure of the protein is shown in Figs. 14 and 17-a by stereoscopic pictures. These two helical segments and heme c show up clearly in the electron density map (Fig.15). The atomic position of the residues 20 through 25, -Val-Glu-Asn-Gly- Gly-Lys-, are shown in Fig.16 together with Fourier map. In the region the conformation of the bonito ferrocytochrome c is different from that of the tuna ferrocytochrome c, and similar to that of the horse ferricytochrome c[30,31] as in Figs. 17-a, b, and c. This structural variation among the molecules in the crystals may be caused by the difference of molecular packing in the crystals. This fact seems to show that the molecule has a few stable conformations in the solution.

Most of the aromatic groups were well defined in the map. The phenyl group of Phe(82) closes the heme crevice in the bonito ferrocytochrome c as in the tuna ferrocytochrome c. The group in the horse ferricytochrome c, however, is exposed to outside of the molecule. The indole group of Trp(59) is favorable to bind to the propionic group of the heme through a hydrogen bond as that of the tuna ferrocytochrome c.[30,31] The orientation of the group in the bonito ferrocytochrome c is schematically shown in Fig.13.

The amino group of Lys(99) seems to bind to carboxylic group of Glu(61) as in Fig.18. There is not a similar interaction between the groups in the horse ferricytochrome c.

Table 2. Flow diagram for extraction and purification of cytochrome c from bonito heart muscle

Frozen bonito hearts

↓

Remove bonding tissues.

Mince

Homogenize in a waring blender for 5 sec. with three volumes of 0.3% $Al_2(SO_4)_3$.

Add 5N H_2SO_4.

Stand for 2 hours at below 10°C.

Filter using a suction bottle.

Extract

↓

Add aqueous NH_3 to pH 8.2 — 8.5.

Filter with the aid of 10g celite per liter of the extract.

Add acetic acid to pH 7.5.

Pass through a column of Amberlite IRC-50.

Scrape off the red part of the resin and wash with ten fold of 0.02M ammonium phosphate buffer(APB,pH7.5)

Elute with 0.05M APB containing 0.5M NaCl(pH 7.5).

Add minimal amount of $K_3Fe(CN)_6$.

Add solid $(NH_4)_2SO_4$ to 50% saturation.

Centrifuge at 8,000 r.p.m. for 20 min.

Supernatant solution

↓

Desalt by passing through a column of Sephadex G-25.

Wash with 0.02M APB.

Elute with minimal amount of 0.05M APB containing 0.5M NaCl.

Desalt by passing through a column of Sephadex G-25.

Pass through a column of Amberite IRC-50(pH 7.5).

Charged column

↓ Develop with 0.2 or 0.25M APB (pH 7.5).

Cytochrome c fraction

↓ Concentrate by the same method as the first chromatography, and elute with 10% saturated ammonium sulfate solution (pH 8.0).

Concentrated cytochrome c solution

Table 3. Flow diagram for the crystallization of bonito ferrocytochrome c

10 ml of 7% ferricytochrome c solution

↓ Add finely powdered $(NH_4)_2SO_4$ to 60% saturation.

Add 5 fold molar excess of ascorbic acid.

Bring the pH to 8.2-8.5 aqueous NH_3.

Add finely powdered $(NH_4)_2SO_4$ in small portions until a faint turbidity appears.

Cetrifuge at 8,000 r.p.m. for 20 min.

Supernatant solution

↓ Add finely powdered $(NH_4)_2SO_4$ in small portions until a faint haze appears.

Cool the solution in ice-water and dissolve the amorphous turbidity.

Repeat the above two procedures till uniform, cotton-like amorphous turbidity appears.

Keep at room temperature without any mechanical shock.

Large crystals after 1 to 2 weeks

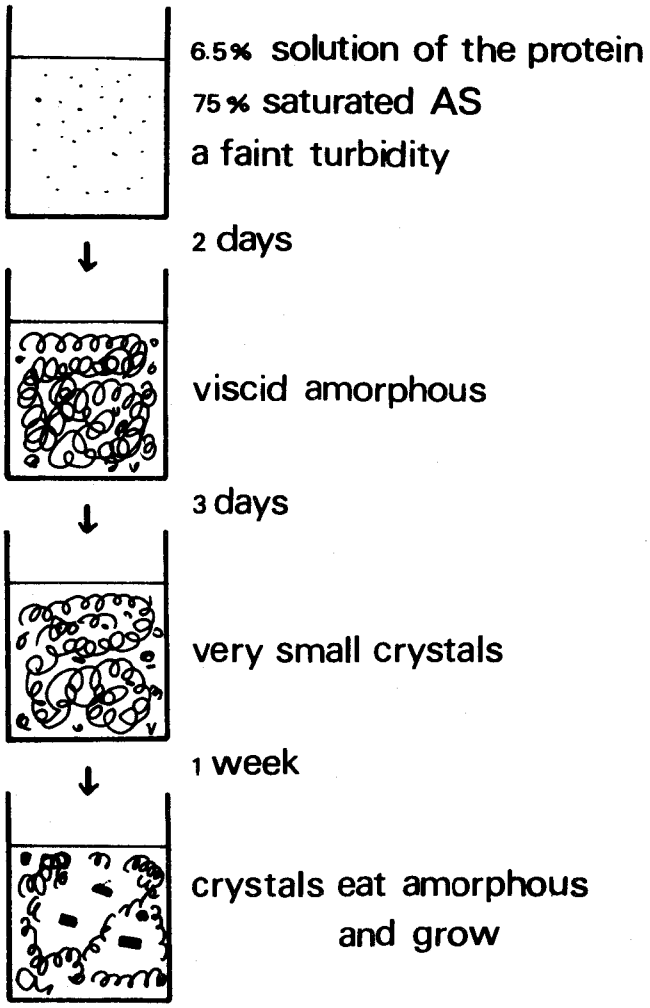

Fig. 6. The pathway of crystal growth. About 10 ml of the protein solution containing 5 fold molar excess of ascorbic acid is added powdered $(NH_4)_2SO_4$ to 60% saturation and the pH of the solution is brought to 8.2-8.5 with conc. NH_3. Another finely powdered ammonium sulfate is added in small portions until a faint turbidity appears. The solution is kept still at about 20°C. After a few days viscid amorphous substance appears. It takes another few days until very small crystals are found. The crystals grow and the amorphous disappears gradually. After one week or more the viscosity of the solution decreases and the crystal growth stops.

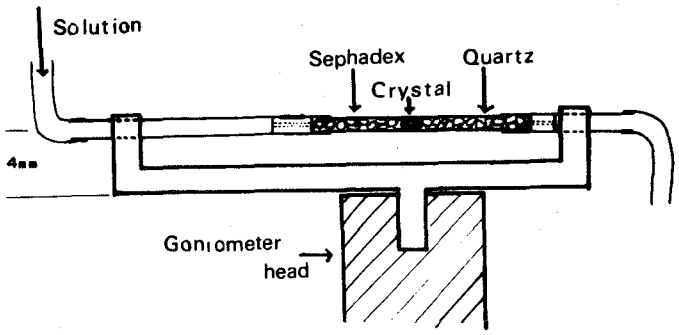

Fig. 7. A modified flow cell. A crystal in a quartz capillary is fixed by Sephadex G-25 coarse. Soaking solution is flowed in the capillary.

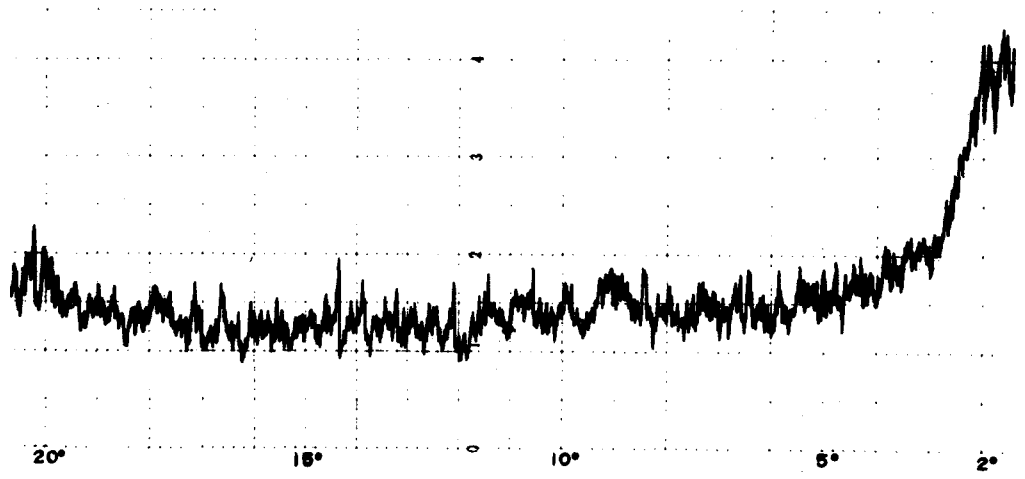

Fig. 8. The background scattering from the flow cell filled with the Sephadex chunks and 87% saturated ammonium sulfate solution.

Table 4. Preparation of isomorphous derivatives

reagents	concentration*	soaking period
$K_3UO_2F_5$	100mg/5ml	2 days
$(CH_3)_2SnCl_2$	3mg/5ml	4 days
$Pt(SCN)_6$	5mg/5ml	5 days
K_3IrCl_6	50mg/5ml	5 days
K_2PtCl_4	1.2mg/5ml	6 days
K_2HgI_4	0.1mg/5ml	8 days

* The concentration of reagents in 87% saturated ammonium sulfate solution containing a small amount of ascorbic acid.

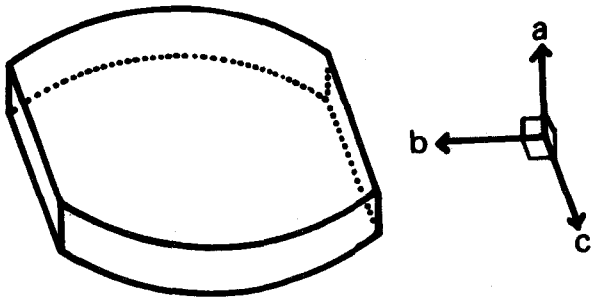

Fig. 9. Crystal shape of the bonito ferrocytochrome c and the orientation of axes.

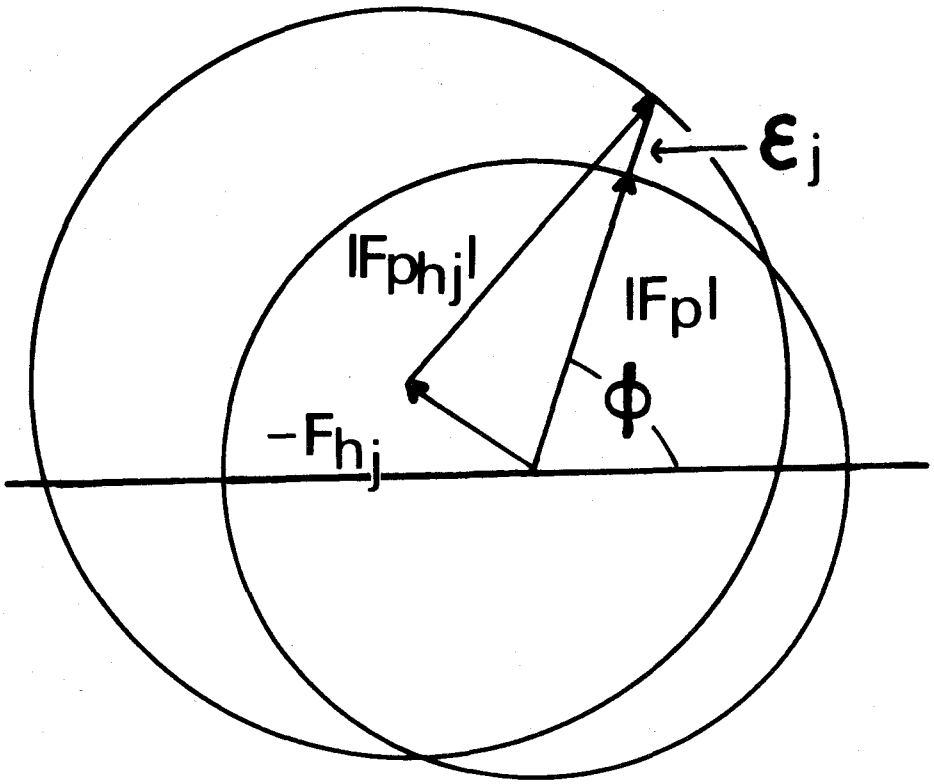

Fig. 10. The relationship between the structure factors of native crystal and derivative one. Where $|Fp|$ and $|Fph_j|$ represent the structure amplitudes of the native and j-th derivative crystals, Fh_j is the structure factor for the heavy atoms in the derivative, ϕ is the phase angle of the native, and ε_j is a lack of closure.

Table 5 Final parameters of heavy atom derivatives

	x/a	y/b	z/c	B	occopancy
$K_3UO_2F_5$-derivative (ΔB=0.390)					
U-1	0.08862	0.13113	0.04700	26.30	41.8
U-2	0.58833	0.14118	0.08073	25.77	70.5
$(CH_3)_2SnCl_2$-derivative (ΔB=-0.400)					
Sn-1	0.88693	0.24386	0.05111	13.94	12.3
Sn-2	0.35445	0.47465	0.17323	13.96	5.7
Sn-3	0.81728	0.44594	0.19766	12.03	62.6
K_3IrCl_6-derivative (ΔB=0.020)					
Ir-1	0.42400	0.26500	0.21400	15.00	13.5
Ir-2	0.93433	0.26077	0.20620	15.00	13.4
K_2PtCl_4-derivative (ΔB=5.400)					
Pt-1	0.24179	0.27008	0.23432	12.30	28.2
Pt-2	0.78346	0.26303	0.17378	13.80	33.2

	Rk			Rc		
	3.0-2.3	-3.0	-4.0A	3.0-2.3	-3.0	-4.0A
$K_3UO_2F_5$	5.7%	4.6%	5.0%	54%	40%	35%
$(CH_3)_2SnCl_2$	9.3	7.5	7.6	69	61	56
K_3IrCl_6	5.0	3.8	3.8	76	63	57
K_2PtCl_4			6.9			51

Where Rk and Rc represent Kraut's R and centric R, respectively.

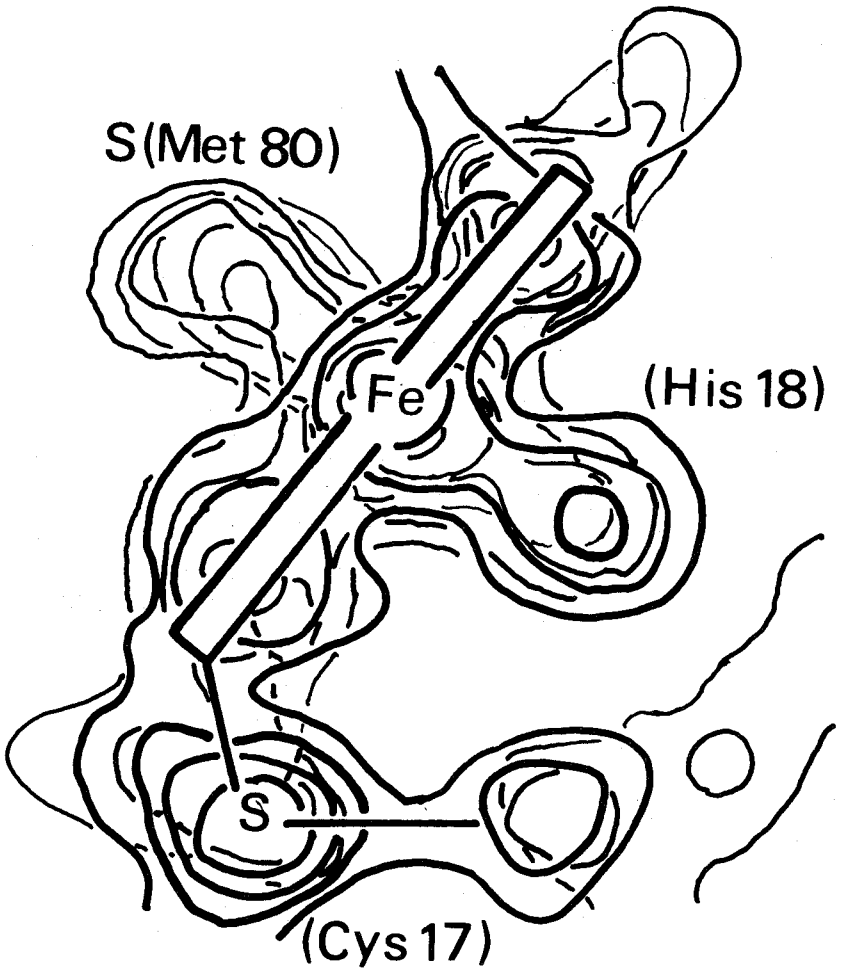

Fig. 11. A composite drawing of three successive electron density sections near the heme iron. The contours are drawn in an arbitrary scale. The iron shows up at the peak of 2.3e/$\AA^3$. The location of 5th (His 18) and 6th (Met 80) ligands, and the sulfur atom of Cys(17) are also clearly indicated with high electron density peaks.

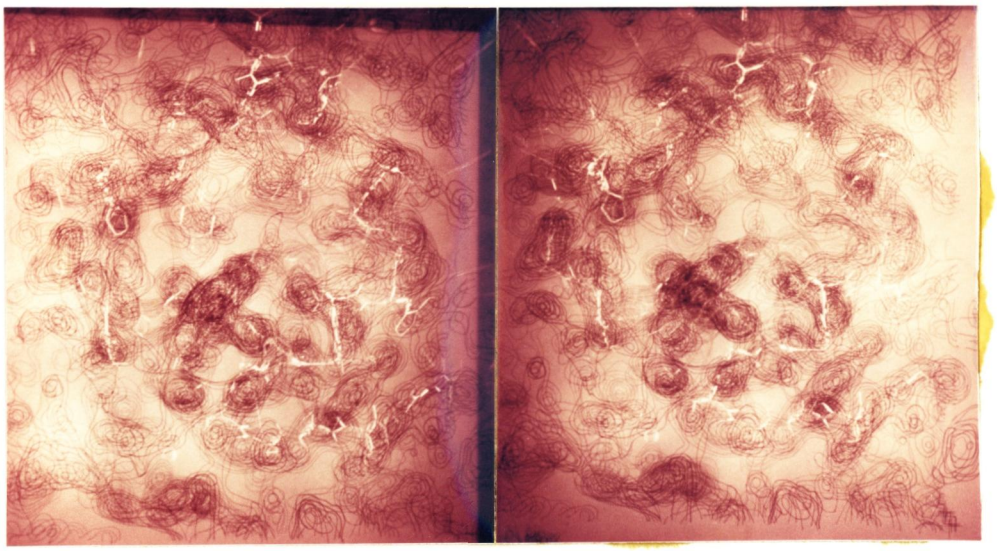

Fig. 12. Stereoscopic drawing of electron density contours (Z=9/38-17/38) with Kendrew-like model, looking down from the top of the molecule. Redish part of the model shows heme. Four pyrrole rings, 5th and 6th ligands clearly appear in the map.

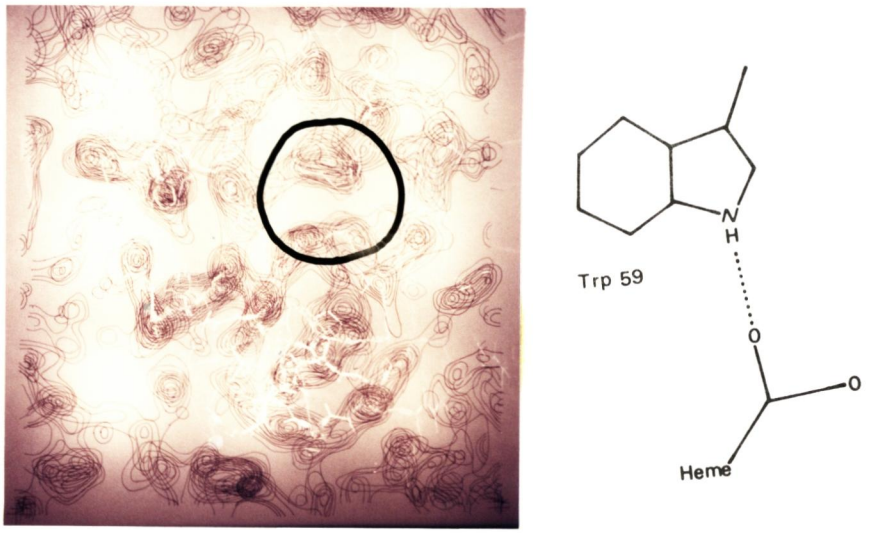

Fig. 13. A composite electron density contours (Z=14/38-17/38) with the model. An indole ring of Trp(59) bound to a propionic group from the heme is clearly revealed in the contours.

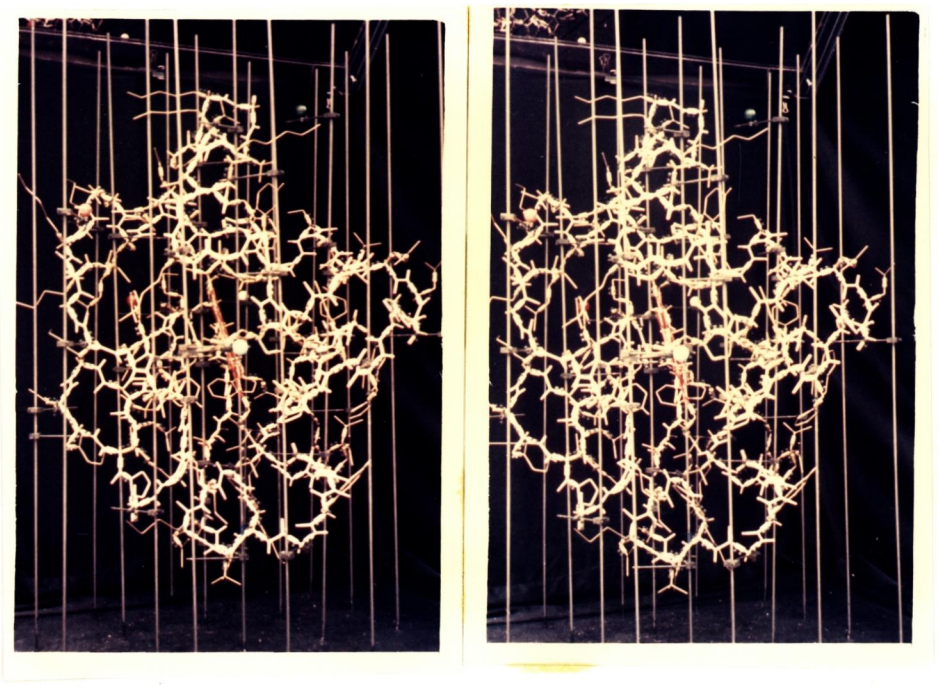

Fig. 14. A pair of stereoscopic pictures of the model. Two helical segments are in the upper part of the molecule. Small colored balls represent heavy atoms bound to the protein in derivative crystals.

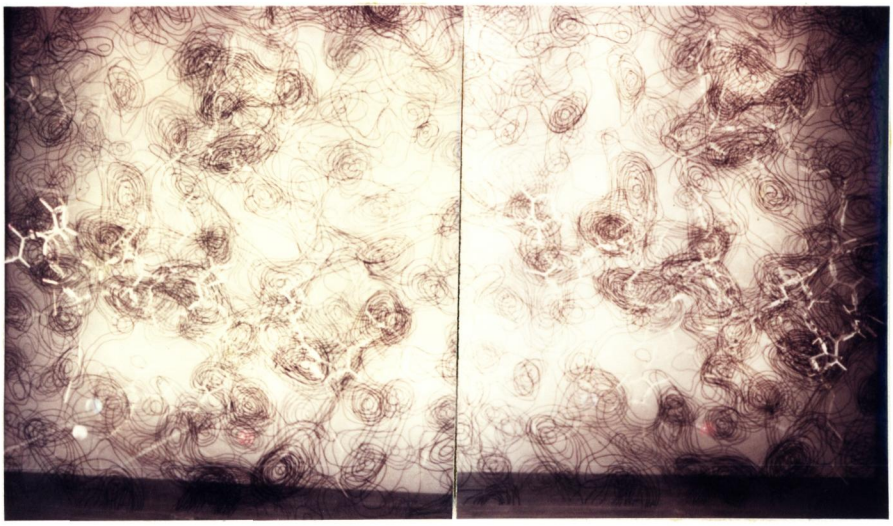

Fig. 15. Stereoscopic drawing of electron density contours (Z=-1/38-4/38) with the model. A helical segment at carboxyl terminal is clearly shown by specific contours.

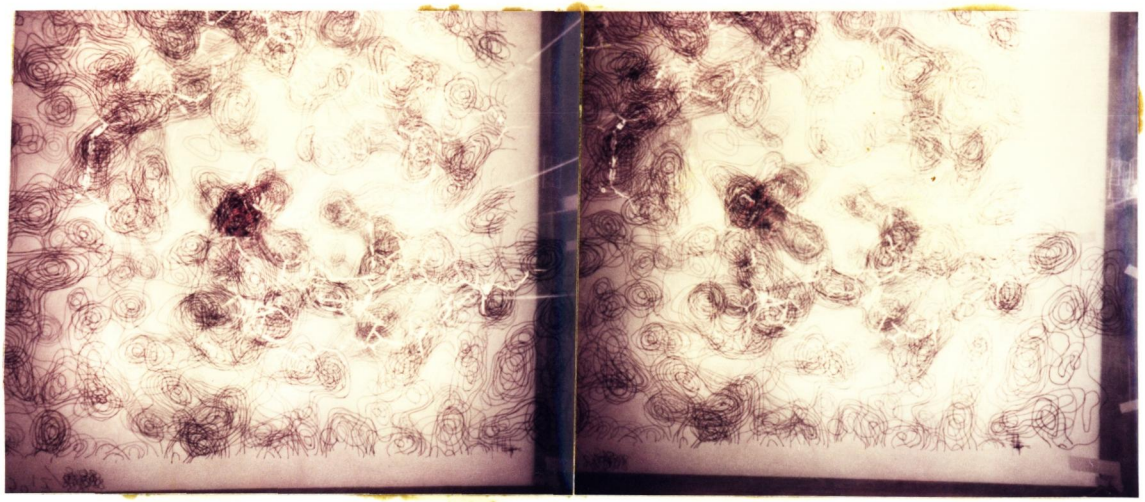

Fig, 16. Stereoscopic drawing of electron density contours (Z=6/38-14/38) with the model. The residues 20 through 25, -Val-Glu-Asn-Gly-Gly-Lys-, are clearly shown in the map.

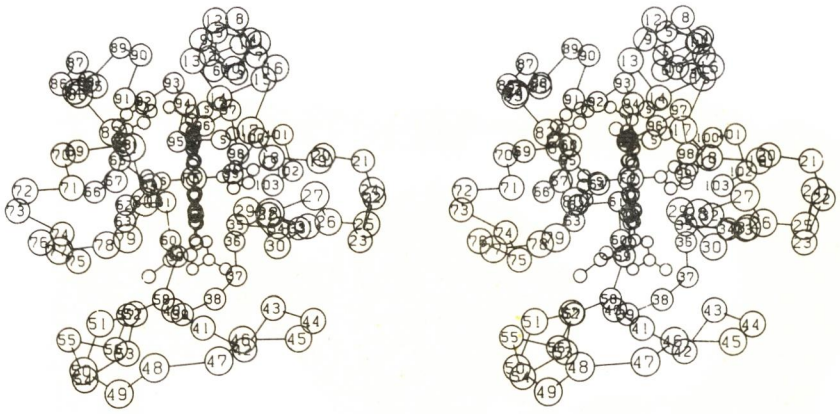

Fig. 17-a. Stereoscopic drawing of the backbone of the bonito ferrocytochrome c. Large circles represent α-carbons and iron, and small ones are some other atoms. The conformation of the residues 20 through 25 is different from the tuna ferrocytochrome c. The phenyl ring of Phe(82) is buried in the heme crevice.

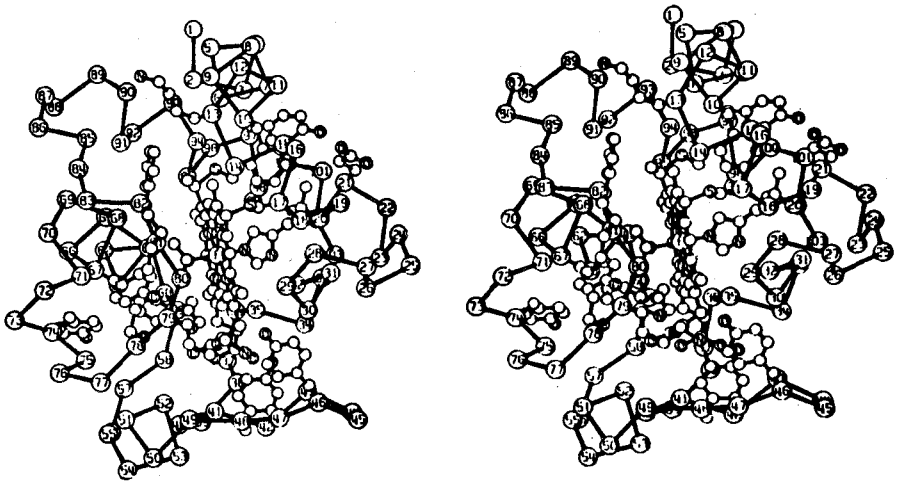

Fig. 17-b. The structure of the tuna ferrocytochrome c.[47]

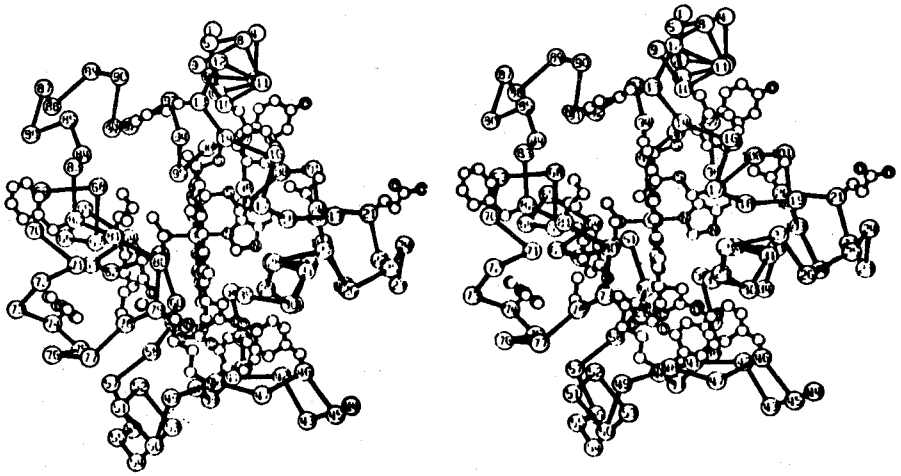

Fig.17-c. The backbone of the horse ferricytochrome c.[29] The phenyl ring of Phe(82) is exposed to the molecular surface. The residues 20 through 25 are in the same conformational states as the bonito ferrocytochrome c.

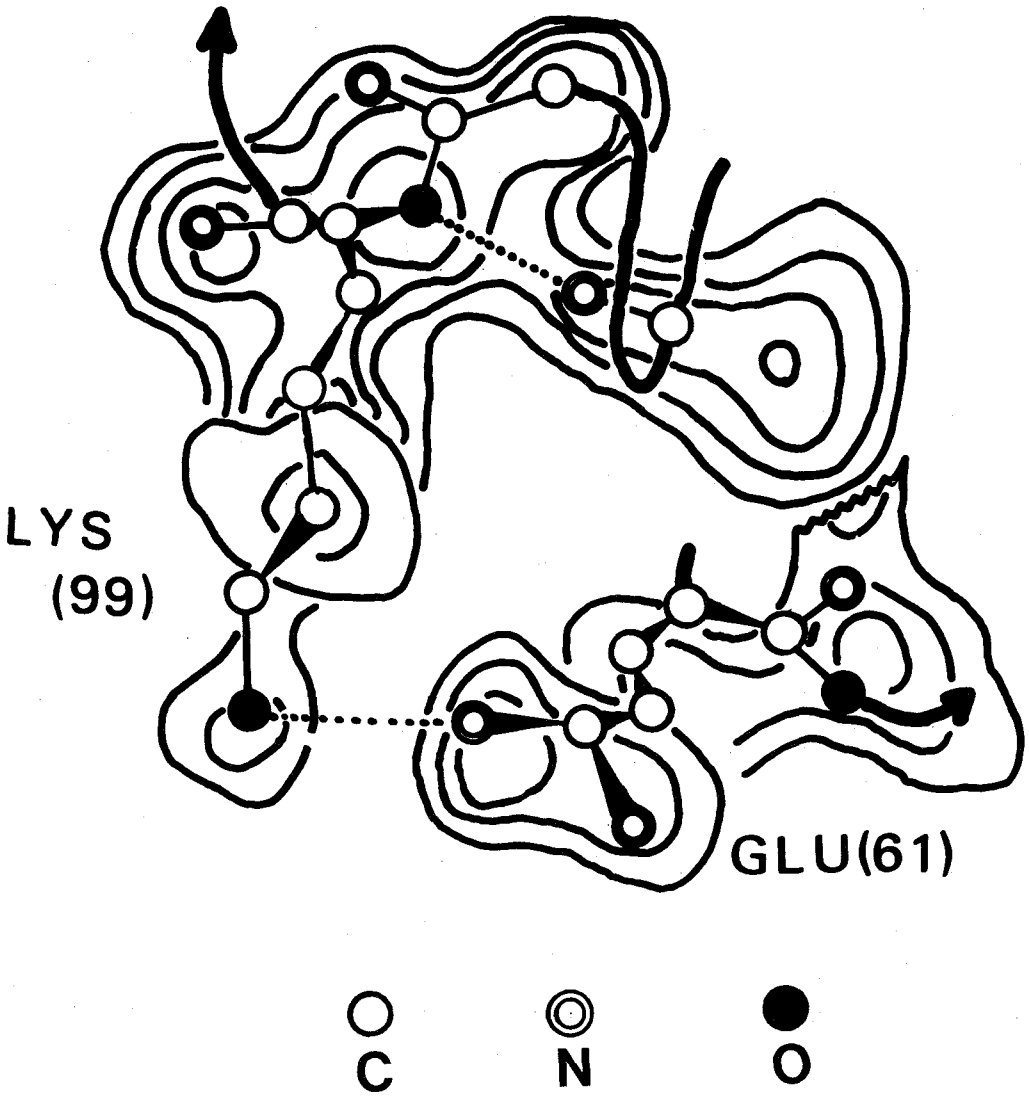

Fig. 18. A part of composite electron density map. Contours are drawn at the interval of 0.30e/Å^3 starting at 0.33e/Å^3. Atomic positions of Lys(99) and Glu(61) are superposed on the map. The broken lines show a hydrogen bond between the amino and the carboxyl groups. The interaction has not been found in the horse ferricytochrome c.

III. Structural change of cytochrome c upon oxidation of the heme iron atom in crystalline state

III-1 Experimental

Oxidation of the crystals

The crystals of ferrocytochrome c have been preserved in the 87% saturated ammonium sulfate solution(87% AS, pH 8.0) containing a sufficient amount of ascorbic acid. The crystals were oxidized by two methods. The oxidation with oxygen molecule (auto-oxidation) was carried out in the solution saturated with oxygen by air-bubbling (pH 5.8). It took fifty days or more before the oxidized molecules were increased to 50% of whole the molecules in the crystal. The oxidation with ferric ion was carried out in the solution of about 10 ml containing a few drop of 0.5M potassium ferricyanide. It took a few days until half of the molecules were oxidized. Auto-oxidation gave more rigid crystals than the oxidation with ferric ion, perhaps because the former seems to change the conformation more gradually than the latter.

The degree of oxidation was estimated by the following formula after the measurement of optical density of α-band at 550mμ,

$$\frac{OD^r - OD^s}{OD^r(1-OD^o/OD^r)}$$

where OD^s is the optical density of the sample solution, OD^r is that after complete reduction with sodium dithionite. In the present case the value of OD^r/OD^o was determined as

3.605 beforehand. The percentage oxidation for three partially oxidized crystals of OXI 1, OXI 2, and OXI 3 were estimated to be 55, 60 and 65%, respectively.

Data collection

Intensity data of about 1,500 and 3,500 reflections were collected at 4Å and 3Å resolutions, respectively, using a four-circle diffractometer. These intensity measurements and absorption corrections for three kinds of partially oxidized crystals were undertaken by the same method described in the previous section. These crystals may be isomorphous with the native reduced crystal, because there were no significant differences in cell dimensions. In order to estimate the experimental errors, three set of intensity data were collected from the three reduced crystals (RED 1, RED 2, and RED 3, respectively). RED 1 is the data as used in the previous section.

III-2 Change of observed structure amplitudes by oxidation of the crystal

The similar change of the structure amplitude was given by the two methods of oxidation of the crystal.

The degree of change of the structure amplitudes observed on the oxidation are summarized in Table 6, and the intensity distribution of (0k0) for each oxidation state (RED 1, OXI 1 and OXI 3) is also shown in Fig.19. This change in the structure amplitudes may be due to the oxidation of the protein, because the difference in the structure amplitudes

is proportional to the oxidation degree as in Table 6 and Fig.19. During the air-bubbling into the soaking solution, the concentration of ammonium sulfate might be increased due to the evaporation of a small amount of water. But the increased concentration does not seem to disturb the distribution of intensity, because the amplitude did not change in the reduced crystal soaked in 100% AS solution (pH 5.5) instead of 87% AS.

III-3 Theory of difference Fourier synthesis

The difference Fourier synthesis is calculated with the coefficient,

$$(|Fph|-|Fp|)\exp(i\phi p)\ ,$$

where Fp is the observed structure factor of the native crystal, and Fph is that of the modified crystal whose electron density is a little different from that in the native crystal, and ϕp is the phase angle of the native crystal (see Fig.20). The coefficient can be rewritten as follows,[32,33]

$$(|Fph|-|Fp|)\exp(i\phi p)=(|Fh|\exp(i\phi h)+|Fh|\exp(i(2\phi p-\phi h)))/2$$

$$=Fh/2+(|Fh|\exp(i2\phi p)\exp(-i\phi h))/2.$$

The Fourier transform (F.T.) of the first term gives the difference electron density between the modified and the native crystals. The F.T. of the second term is the convolution of the inverse of the F.T. of the first term and the F.T. of $\exp(i2\phi p)$. The latter gives sometimes small but systematic error. However, the Fourier synthesis has been carried out successfully to reveal the difference in the

electron density. In the present case Fp is nearly equal to Fph, so that the error may be negligible.

III-4 Difference electron density between the oxidized and the reduced crystals.

Five difference maps were calculated at 4Å resolution. They were OXI1-RED1, OXI2-RED1, OXI3-RED1, RED2-RED1, and RED3-RED1. And at 3Å resolution, three difference maps of OXI2-RED1, RED2-RED1, and RED3-RED1 were synthesized. These difference density were computed using above coefficient weighted by individual figure of merit to minimize the errors due to the ambiguity of phase angles of the native crystal. Some details of the maps are summarized in Table 6. To avoid the confusion of the reasonable peaks with noises, all these maps were compared with one another, and the noise levels were estimated by

$$\Delta\rho\max\langle\Delta\mathrm{Foxi}\rangle/\langle\Delta\mathrm{Fred}\rangle,$$

where $\Delta\rho\max$ is the maxmum peak height in the difference map between two reduced crystals, and $\langle\Delta\mathrm{Foxi}\rangle$ and $\langle\Delta\mathrm{Fred}\rangle$ are averaged differences of structure amplitudes between the reduced (RED 1) and the oxidized crystals, and between the reduced (RED 1) and the other reduced crystals, respectively. The difference maps between the oxidized crystals and the reduced one (RED 1) give only one reasonable peak at (0.43 0.26 0.21) whose height satisfies following two conditions,

(1) The peak is higher than the noise level in all the difference maps between the oxidized and the reduced crystals.

(2) The peak has the same sign in all the difference maps. The peak at (0.43 0.26 0.21) is as high as 0.045(OXI1-RED1), 0.065(OXI2-RED1), and 0.115e/Å^3(OXI3-RED1), respectively, for 4Å resolution, and 0.135e/Å^3(OXI2-RED1) for 3Å resolution. Fig.21 shows the peak in the map at 3Å resolution. There is no negative region which is comparable to this prominent peak in these maps, so that the peak may indicate a newly fixed substance from the solution in the crystal. Judging from the shape and size of the peak, it may be due to a sulfate anion. This is consistent with the result from the biochemical experiment which shows the oxidized protein binds one more anion such as a chloride anion than the reduced protein.[21)]

The sulfate anion is in the same region as the carboxyl group of Glu(61) of the reduced crystal which is bound to the amino group of Lys(99) in the reduced crystal, so that the carboxyl group seems to move elsewhere by the oxidation of the crystal. The movement of the carboxyl group could not be indicated in the difference maps, because the peak height of the carboxyl group is expected to be lower than the noises in the difference maps. The expected height of the peak is estimated as follows,

$$\Delta\rho(SO_4^{=})e(CO_2^{-})/e(SO_4^{=}),$$

where $\Delta\rho(SO_4^{=})$ is the peak height of the sulfate anion in the difference map, $e(CO_2^{-})$ and $e(SO_4^{=})$ are electron numbers contained within the carboxyl and the sulfate groups, respectively. The expected value is 0.051e/Å^3 for the difference map of (OXI2-RED1) at 3Å resolution.

In other regions, there is no significant difference density in the maps. This fact shows that the molecule oxidized in crystalline state may be in a different conformational state from the horse ferricytochrome c, and that the molecule may be in a conformational state intermediate between ferro- and ferricytochrome c in the solution.

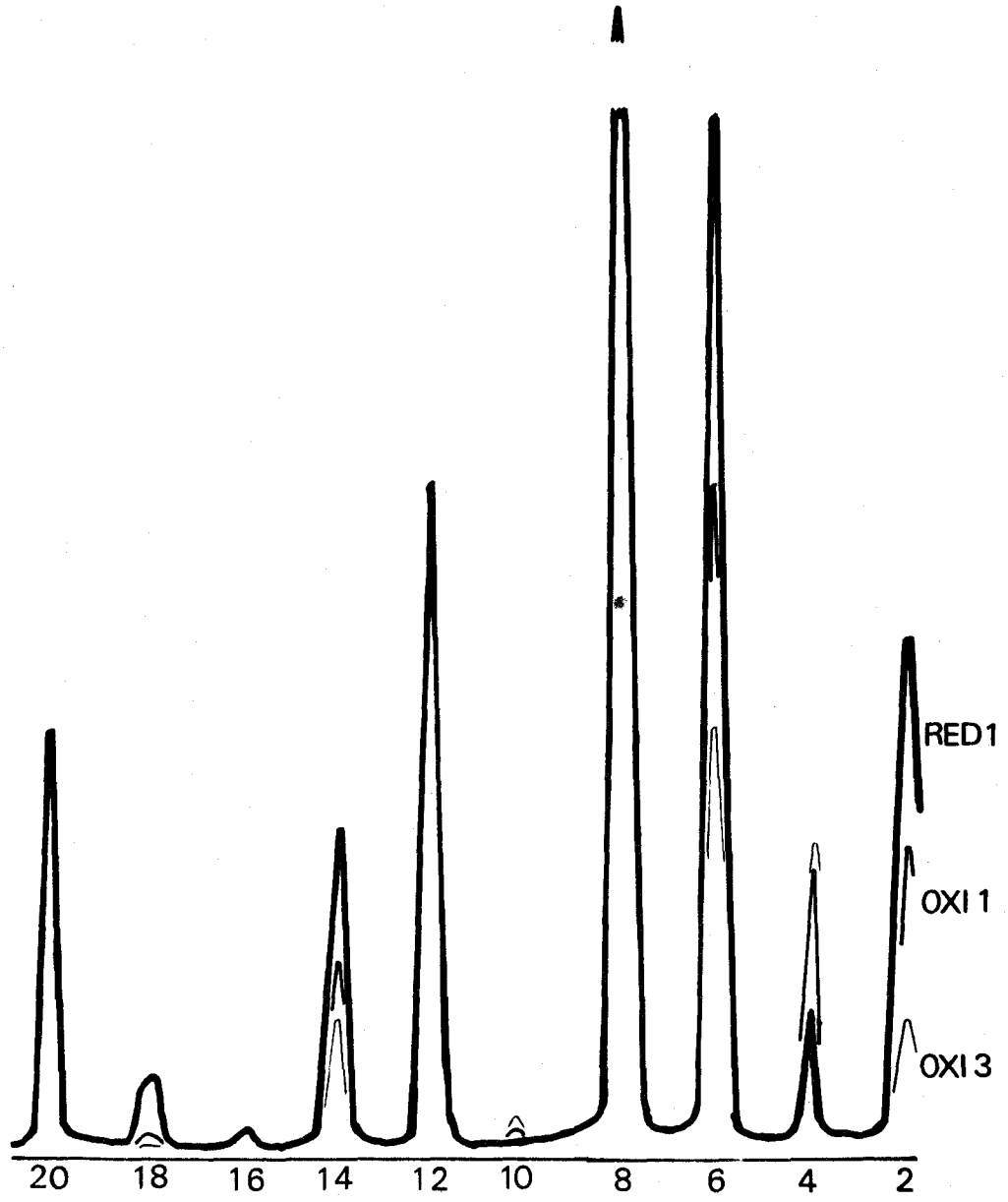

Fig. 19. Intensity change for (0k0) reflections upon oxidation of the crystal. Heavy line shows the profile of the reduced crystal(RED 1), other thin lines are those of the oxidized crystals(OXI 1 and OXI 3). The higher oxidation ratio is, the larger intensity change is.

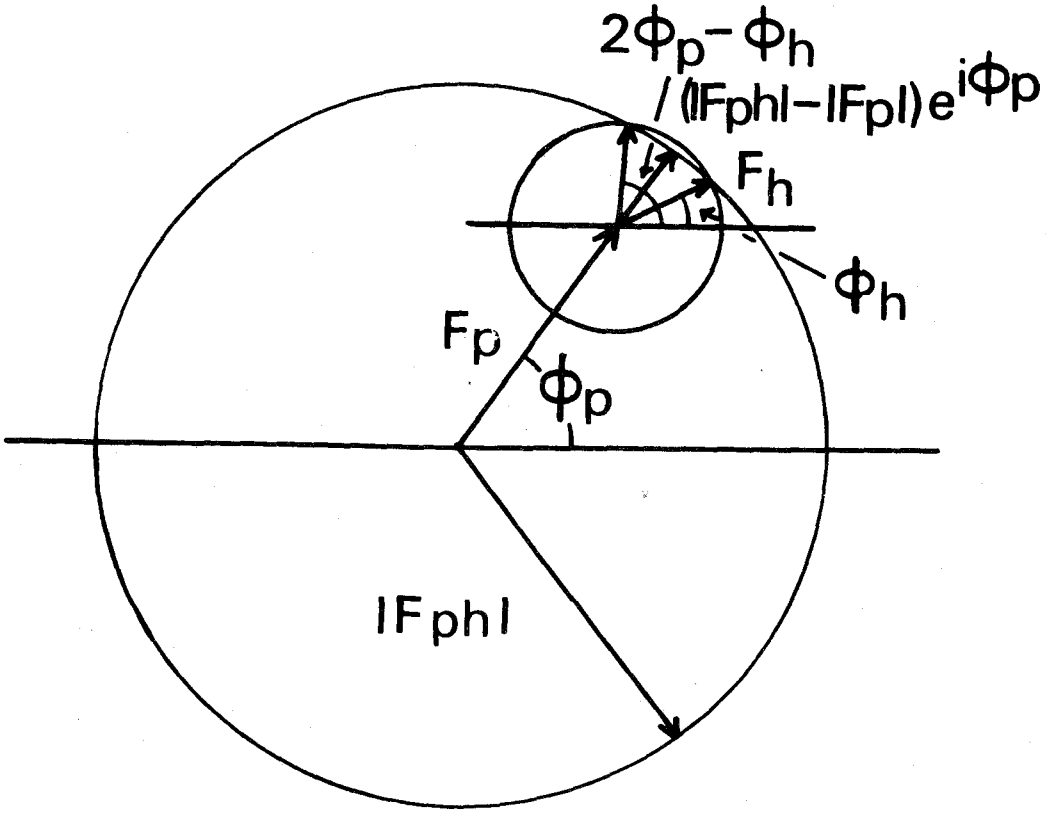

Fig. 20. A difference Fourier synthesis in the general non-centrosymmetric case. $(|Fph|-|Fp|)\exp(i\phi p)$ is the coefficient. Where $|Fp|$ and ϕp represent the structure amplitude and the phase angle of the native crystal, and $|Fph|$ is the structure amplitude of the derivative, and ϕh is the phase angle of the structure factor of the difference electron density between the derivative and the native crystals.

Table 6. Summary of difference Fourier syntheses

	percentage oxidation	$\langle\|\Delta F\|\rangle/\langle\|F\|\rangle$ *1)	highest *2) peak	other *3) peak	noise *4) level
4Å resolution					
OXI 1	55%	5.1%	0.045e/Å^3	0.045e/Å^3	0.042e/Å^3
OXI 2	60	5.6	0.065	0.055	0.046
OXI 3	65	7.6	0.115	0.060	0.062
RED 2	20	2.6	0.012	0.022	
RED 3	20	2.7	0.012	0.022	
3Å resolution					
OXI 2	60	7.4	0.135	0.070	0.067
RED 2	20	3.4	0.015	0.030	
RED 3	20	3.3	0.020	0.030	

*1) $\langle|\Delta F|\rangle$ is the averaged value of the difference of structure amplitude between the oxidized and the reduced crystals, $\langle|F|\rangle$ is the averaged value of the structure amplitude of the reduced crystal.

*2) Electron density at (0.43 0.26 0.21) in the difference map. The highest peak in the difference map between the oxidized and the reduced crystals is appears at this position.

*3) The next highest peak in the difference map between the oxidized and the reduced crystals, and the highest peak in the difference map between two reduced crystals.

*4) The values were estimated by the formula described in section III-4.

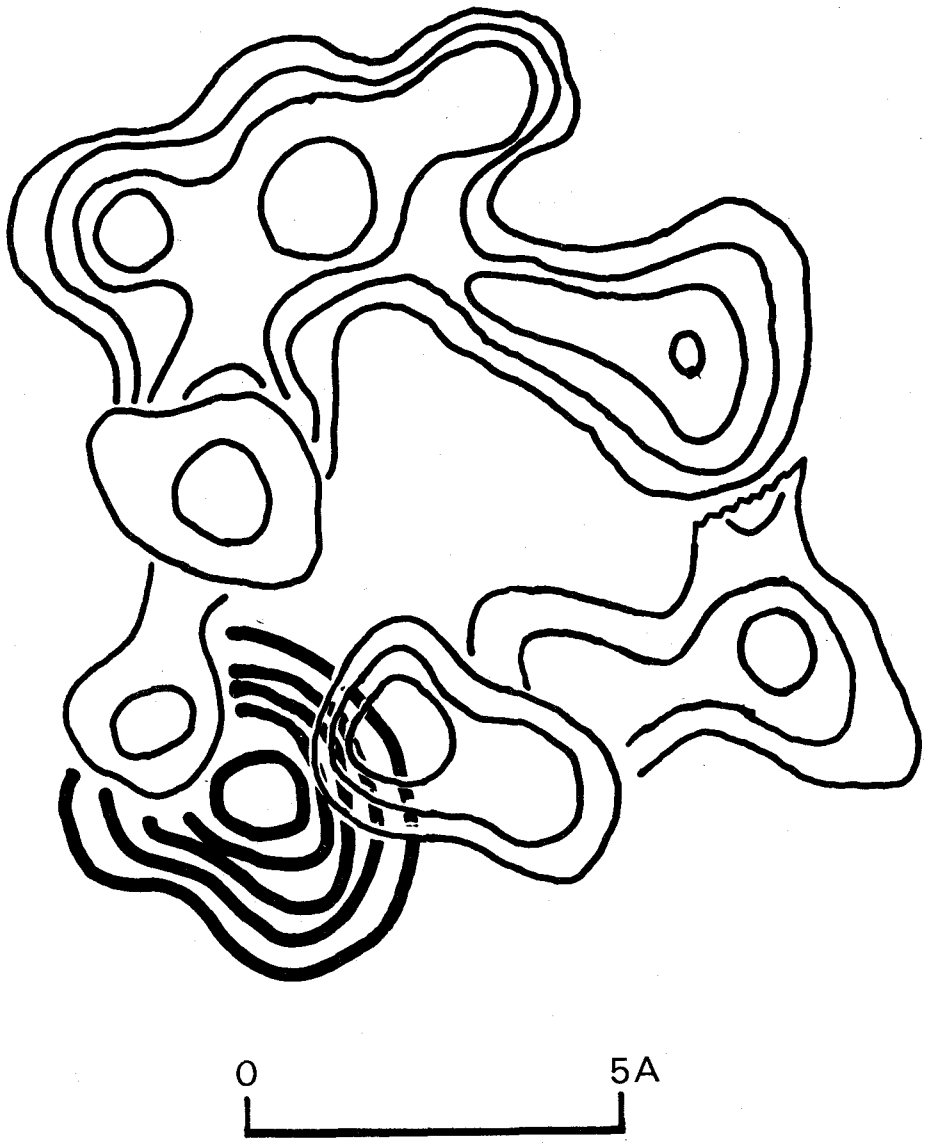

Fig. 21. A part of composite difference electron density map of OXI1-RED1 at 3Å resolution (heavy lines), together with the normal electron density contours which are also shown in Fig.18. The contours for the difference map are drawn at intervals of 0.025e/Å^3, starting at 0.025e/Å^3.

IV. Discussion

An electron removed from substrates in a respiratory chain is not directly transferred to oxygen but through flavoproteins, cytochromes and other substances as described in the first section. The electron transfer is conjugated with ATP synthesis at three sites in the respiratory chain and seems to couple with other physiological functions. In this respect it is interesting to show the relationship between the oxidation-reduction mechanism of cytochrome c and the tertiary structure.

IV-1 Oxidation-reduction mechanism of cytochrome c

Cyclic oxidation-reduction

It has been indicated in the previous section that the bonito and the tuna ferrocytochrome c's are in different conformational states from each other, and that the protein oxidized in crystalline state is also in a different conformational state from that of the horse ferricytochrome c. These structural differences are summarized in Table 7. These facts suggest that the protein is able to have several conformations within each oxidation state.

The twenty-one percent of the conservative residues of the protein are glycine. This unusually high content of glycine residues compared with other proteins seems to enable the protein to be in multiple conformational states within each oxidation state, because a glycine residue increases flexibility of a main chain. Especially the residues 23, 24, 34, 37, 45, 56, 77 and 84 seem to be important for the

main chain fluctuation. The residues of 29 and 41, however, cannot rotate the main chain due to the steric hindrance with the heme group. The residues 6 and 89 are in the helical regions so that the rotation about the residues is almost impossible. The main chain flexibility is schematically shown in Fig.22. In the region including the residues of 23 and 24 the conformational difference was observed between the bonito and the tuna ferrocytochrome c's, and the migration of Phe(82) at the near site of Gly(84) was also revealed crystallographically.

The presence of the multiple conformational states is also supported by the following experiments. The ferricytochrome c is cyanized and carbon-monoxidized at room temperature, however, the ferrocytochrome c reacts with cyan and carbon-monoxide only at high temperature.[18] The reduced protein at high temperature, therefore, may be in the similar conformational state to that of the ferricytochrome c. Within the oxidized state two different conformational states have been also reported,[34] they are called "cold type" and "hot type", respectively. In physiological condition 6% of ferricytochrome c are "hot type" whose entropy is higher than "cold type" by 43.2 entropy unit per mole.[34] The reduced protein is in lower entropic state than the oxidized. In a course of the reduction of ferricytochrome c by chromous ion, the conformational change to lower entropic state is followed by the reduction of the heme iron.[35]

These multiple conformational states suggest "cyclic oxidation-reduction" mechanism as shown in Fig.23. Where

the change of the conformational state and the electronic one do not occur at the same time, one of them is followed by the other. In Fig.23 "R" and "O" represent the conformations of the reduced and the oxidized states, respectively, "R" and "O'" represent the conformations similar to the reduced and the oxidized states, and the iron atoms are in the ferric and ferrous states, respectively. The conformational states of "R" and "O" may be in an equilibrium state of two or more conformations. There are two possible oxidation schemes. One of them is "R$\longrightarrow$ R'$\longrightarrow$ O", and the other is "R$\longrightarrow$ O'$\longrightarrow$ O", in the former scheme the change of electronic state is followed by the conformational change, whereas in the latter case the structural change is followed by the oxidation of the iron atom. At the present stage it cannot, however, be described which is a reasonable mechanism for the oxidation. Similar procedure can be proposed for the reduction scheme of the protein. The fact that the conformational change is followed by the electronic change of the iron upon the reduction by the chromous ion[35] shows that the reduction scheme is "O$\longrightarrow$ O'$\longrightarrow$ R" in this case.

In the cyclic mechanism the conformational change of the protein must be concerted with the change of electronic state of the iron atom. In the physiological condition cytochrome c is in contact with other proteins such as cytochromes c_1 and a. The concerted change of the conformational state and the electronic one of cytochrome c may be effectively caused by the inter-molecular interaction among these proteins.

Pathway of an electron at reduction

Another question about the mechanism of the oxidation-reduction of the protein is what residues of the molecule mediates the electron transfer between the molecular surface and the iron atom. As described in the previous section cytochrome c accepts an electron from cytochrome c_1 and donates the one to cytochrome a (Fig.5). It has been generally agreed with biochemical experiments[36,37] that the passage of an electron through the mammalian cytochromes cannot take place by direct interaction between heme groups. This conclusion appears to be substantiated by the structural investigations of cytochrome c which show that the heme group is buried in the molecule in both oxidation states[38,39].

Some authors have been discussed whether the intermolecular electron transfer is accomplished through a single surface site of cytochrome c molecule or not. Chance and Williams[40] had suggested that a single acceptor area can perform the function of accepting and donating an electron by rotation of the molecule (Fig. 24). Okunuki, on the other hand, proposed that one path from the surface to the heme iron atom is not sufficient in the cytochromes which are fixed with a neighbour in the respiratory chain as in the particles of Pseudomonas cytochrome oxidase.[41] This is supported by a few experiments. A chemical modification of the protein does not block the oxidase activity but the reductase activity.[42,43] The binding of an antibody to the protein disturbs only the oxidase activity.[44]

In cytochrome $\underline{c}_2$ molecule which resembles cytochrome $\underline{c}$ in tertiary structure, a single path of a electron flow upon the oxido-reduction has been proposed from crystal structue investigation.[45] The different mechanism of the electron transfer, however, may be permissible among those of cytochromes $\underline{c}$ and $\underline{c}_2$, because cytochrome $\underline{c}$ is in contact with the protein molecules such as cytochromes $\underline{c}_1$ and $\underline{a}$, whereas the cytochrome $\underline{c}_2$ appears to interact with a bacteriochlorophyll $\underline{a}$ molecule whose chemical formula is as follows.

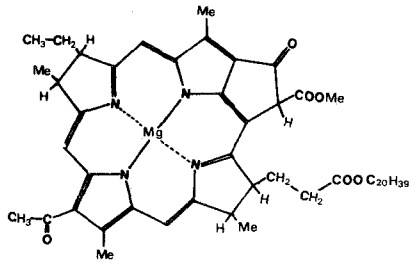

From these facts it should be concluded that an electron is transferred by different pathways in cytochrome $\underline{c}$ molecule on the oxidation and reduction.

Recently Myer reported several results from the specific modification of Trp(59) with N-bromosuccinimide (NBS) as follows,[42,43]

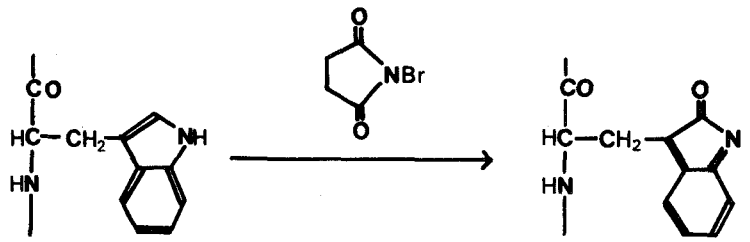

The modification does not decrease the succinate oxidase activity but NADH reductase activity. He found no differences between the native and the modified cytochrome $\underline{c}$'s except in

the Soret CD band, suggesting that the chemical structure change causes small but significant conformational change of the prothetic group or its vicinity, and the electronic interaction of the heme and protein chain is altered by the conformational change.

As described in the previous sections, the evolutionally invariant residue of Trp(59) is bound to the propionic group of the heme through a hydrogen bond (Fig.16), and migrates during the oxidation and reduction of the protein.

These facts suggest that Trp(59) plays an important role in the reduction of cytochrome c. These may be two possible ways, that is,

1. the indole ring plays a key role in constructing the pathway of an electron from the surface to the iron atom, for instance by hydrogen bond network,
2. the indole ring itself is in the pathway of an electron, for instance by electron transfer as follows.

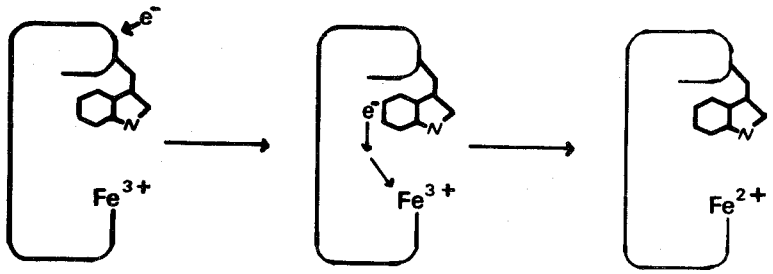

In the first case the chemical modification of the indole ring may disturb the hydrogen bond network in the lower part of the molecule, so that the electron transfer is blocked.

In the second case, an electron transfer from Trp(59) to heme must be disturbed by the oxidation of the indole ring by NBS. This is supported by the molecular orbital calculation which show the energy level of the lowest unoccupied orbital to be lowered by the oxidation as shown in Fig.26. An electron trapped in the lowered orbital of the oxidized indole ring may become impossible to move elsewhere, so that the heme iron is not reduced. The calculations were carried out by a simple LCAO molecular orbital treatment for the π-electron system alone (simple Hückel's method). The sets of Coulomb and exchange integral values suggested by Ladik[46] were used. These are:

$\alpha(C)=\alpha_0$, $\alpha(\rangle C^*-N)=\alpha_0+0.07\beta_0$, $\alpha(\rangle C^*=N)=\alpha_0+0.07\beta_0$,
$\alpha(\rangle N-)=\alpha_0+0.90\beta_0$, $\alpha(=N-)=\alpha_0+0.58\beta_0$, $\alpha(C^*=O)=\alpha_0+0.23\beta_0$,
$\alpha(=O)=\alpha_0+1.30\beta_0$, $\beta(C-C)=\beta_0$, $\beta(C-N\langle)=1.10\beta_0$,
$\beta(C=N-)=\beta_0$, and $\beta(C=O)=2.0\beta_0$,

where α_0 and β_0 are Coulomb integral of the carbon atom and the exhange integral of C-C bond in benzene ring, respectively.

Takano et al. proposed the following sequence of an electron transfer: reductase$\longrightarrow$ Tyr(74)$\longrightarrow$ Trp(59)$\longrightarrow$ Tyr(67) $\longrightarrow$ heme, from the specific location of the aromatic groups and the heme in the ferri- and ferrocytochrome c's (Fig.27). In order to transfer an electron the rotation of the phenol ring of Tyr(74) about C_α-C_β bond seems to be necessary for the overlapping of the π-electron cloud of the ring with that of the indole ring of Trp(59) as in Fig.28. The rotation seems to be possible.

The shortest pathway from the surface to Trp(59) is the way of Glu(61)→ Asn(60)→ Trp(59) whose peptide chain is rather extended. This is one of the possible pathway of an electron. In this case an electron is accepted from the reductase by the carboxyl group of Glu(61) or the peptide bond between the residues 60 and 61. A similar electron transfer mediated by polypeptide chain has been observed in the reduction of N-acetylglycylglycinatopentammine cobalt(III) complex by Cr(II) as follows.[49]

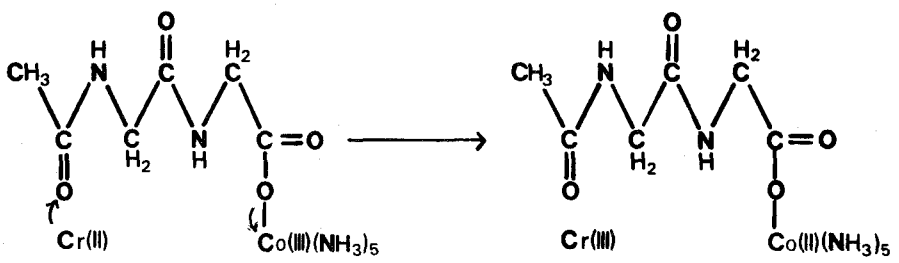

However, it has not yet been indicated that the extended structure of polypeptide chain is favorable for the electron transfer.

With respect to the way of electron flow from Trp(59) to the heme, Myer[43] has been proposed the mechanism of direct transfer from the indole ring to a pyrrole ring of the heme by π-electron overlapping. This Myer's scheme seems to be unreasonable, because the location and the orientation of the indole and the heme planes are not appropriate for π-electron overlapping in both ferri- and ferrocytochrome c's.[30] Another possible mechanism is the electron transfer mediated by the propionic group bound to the indole ring through a hydrogen bond. A weak point of this scheme

is for the pathway to include two methylene group which may disturb the electron transfer.

Another reduction scheme has also been proposed by Kowalsky.[50] In the case of the reduction by chromous ion the reduction seems to be achieved by direct attack of the ion to the sulfur atom of Cys(17) which is exposed to the molecular surface, that is, an electron is transferred from Cr(II) to the iron atom mediated by the exposed sulfur atom and the pyrrole ring "b" as in Fig.30. The scheme, however, may be different from that in the physiological condition.

Degradation of the oxidase activity upon chemical modifications and a possible oxidation mechanism of the protein

The oxidase activity of cytochrome c degrades proportionally to the number of acetylated or succinylated lysyl groups.[51] The succinylation which produces negative charges decreases the activity more effectively than the acetylation which neutralizes positive chage of the group.[51,52] The degree of guanizylation of ε-amino groups which increases positive charges is proportional to the increase of the activity. These facts are shown in Fig.31 and suggest that the positively charged lysyl groups may take part in the complex formation of the protein with cytochrome a whose surface is negatively charged as proposed by Takemori et al.[53] These chemical modifications seem to alter Michaelis constant, $Km=k_{+1}/k_{-1}$, in the following equation.

reduced Cyt.c + oxidized Cyt.a

$$\xrightarrow[k_{-1}]{k_{+1}} \text{(Cyt.c - Cyt.a) complex}$$

$$\xrightarrow{k_{+2}} \text{oxidized Cyt.c + reduced Cyt.a .}$$

Although trinitrophenyl(TNP) modification of lysyl groups also decreases the activity, it is different from the modifications mentioned above in the sense that the first trinitrophenylation gives a drastic degradation of the activity as shown in Fig.31. In this case Lys(13) is modified at first.[51] The result suggests that the modification affects not only the complex formation (Km) but also the second step of the reduction (k_{+2}). As in Figs. 14 and 32, the amino group of Lys(13) is at the vicinity of the phenyl ring of Phe(82) which is converted to outside of the molecule upon the oxidation. The aromatic group of TNP-Lys(13), therefore, is expected to have comparatively stronger interaction than the aliphatic groups such as the acetyl group with the phenyl ring of Phe(82). The interaction appears to disturb the conformational change of Phe(82) on the oxidation with cytochrome a, that is, the sequence of "R⟶ O'" is blocked in the cyclic oxidation-reduction mechanism described previously. This process is shown in Fig.32.

IV-2 Anion catching and its physiological meanings

Anion catching scheme and oxidation mechanism of the protein

In the previous section it has been shown that the ferri-

cytochrome c oxidized in crystalline state catches one more anion than the reduced one. This is schematically shown in Fig.33. In the reduced protein the amino group of Lys(99) is linked to the carboxyl group of Glu(61) by a hydrogen bond. On the other hand the amino group of the oxidized protein is linked to a sulfate anion instead of the carboxyl group of Glu(61). In the residues Trp(59) through Asn(62) the conformational difference of the main chain between two oxidation states has been indicated by the crystal structure analysis of the reduced and the oxidized proteins.[30] The conformational change relating to the electron distribution change in the pyrrole ring "a" is also expected from Myer's results.[42,43]

From these facts two possible ways are considered for the scheme of the conformational and electronic changes of the protein from the reduced to the oxidized state as follows.

Case 1 The hydrogen bond between Glu(61) and Lys(99) in the reduced protein is broken by the attack of a sulfate anion to the amino group of Lys(99), and the structure is converted into a conformation similar to that of the oxidized protein, so that the molecule is easily oxidized. The mechanism is also shown by the following equation.

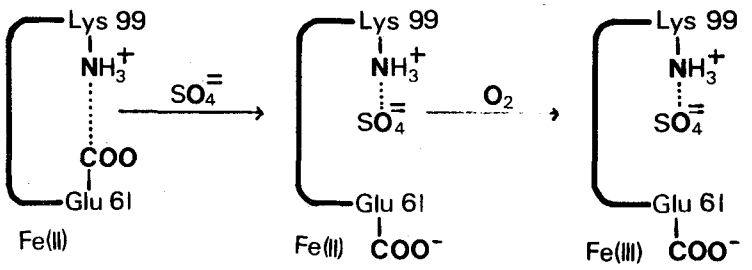

Case 2 As the first step , the heme iron atom is oxidized, and the conformational state changes from the reduced to an oxidized state in which the carboxyl group of Glu(61) is not linked to the amino group of Lys(99). The conformational change enable a sulfate anion to bind to the amino group, as shown in the following equation.

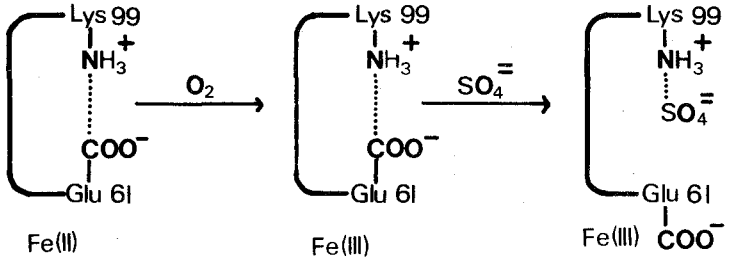

In case 1, the attack of a sulfate anion to the amino group of Lys(99) takes part in the oxidation. This is supported by the result that the auto-oxidation of ferrocytochrome c is substantially hastened by the presence of halogenated carboxylic acid which are more acidic than the carboxyl group of glutamic acid.

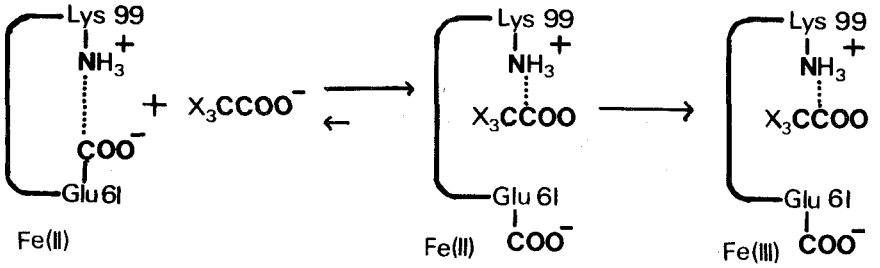

The mechanism is also supported by the experiments reported by Kitahara et al.[54] and by Nicholls.[55] Kitahara et al. showed that a few sulfate anions bind to the oxidized protein and all the sulfate anions are substituted by the same number of phosphate anions. Nicholls reported that the lower

the concentration of phosphate anion, the slower the oxidation velocity of cytochrome c by the oxidase is, in spite of increase of the concentration of the Michaelis complex.

The binding of a phosphate anion to the amino group may be one of the most important step of the oxidation in vivo. Besides the conformational change of Phe(82) may be also very important condition for the oxidation.[31] These two steps may cooperatively take place.

This process may be "R⟶ O'⟶ O" in the cyclic mechanism described before.

Mitochondrial anion transport of cytochrome c

Ferro- and ferricytochrome c's distribute at both sides of intermembrane space and matrix in inner membrane of mitochondria, respectively. The protein adsorbs one more sulfate anion in the oxidized state than in the reduced, and the anion is substituted by the phosphate, as described before.[54] These facts suggest that the protein may be a phosphate carrier in the inner mitochondrial membrane. This assumption appears to be substantiated by the experiment which indicates that the mitochondrial transport of the phosphate anion is blocked by several mercurials which will destroy the tertiary structure of the protein.[58-60] This physiological function as a phosphate carrier is schematically shown in Fig.34.

Oxidative phosphorylation

It is well known that one equivalent of ATP is formed per one atom of oxygen consumed in the oxidation of ferro-

cytochrome c by chytochrome a in the co-existence of O_2.[22,56] The enzymatic mechanism of ATP synthesis, however, has not precisely elucidated.

Recently Young et al.[57] reconstituted the complex of cytochromes a and c, which has a respiratory controle index of 4 without external phospholipid and other factors. The complex seems to be an enzyme of the oxidative phosphorylation. The anion binding site of ferricytochrome c indicated in the present work may be an active site in which the phosphate group is activated for the ATP synthesis. More experiments are, however, necessary to confirm this problem.

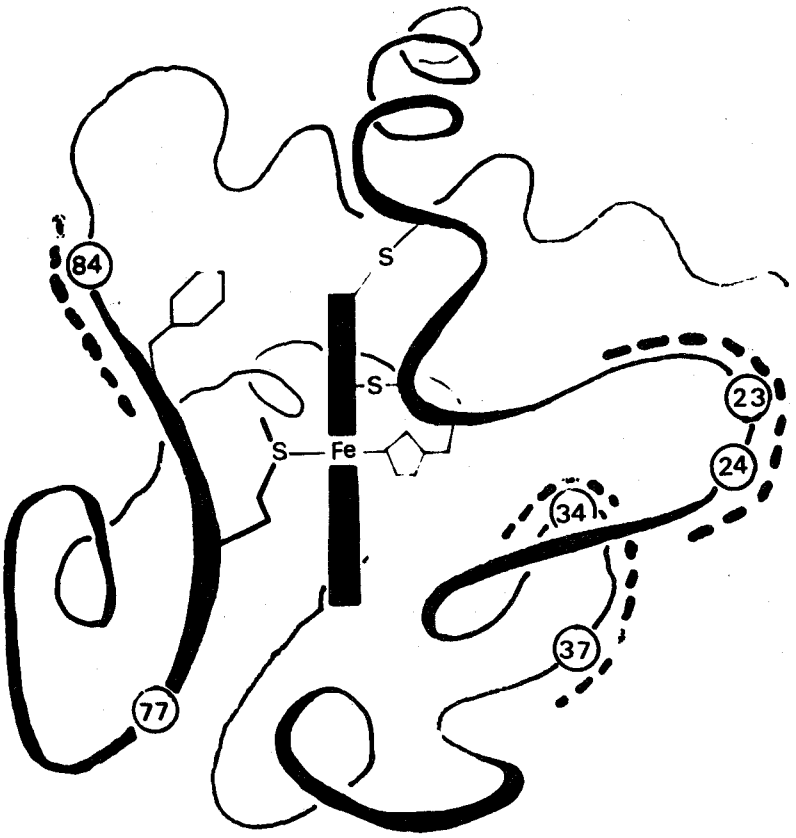

Fig. 22. Main chain flexibility and some conservative glycine residues are shown. Broken lines represent some regions which seem to be flexible. In the regions around 84, and 23 and 24, a few conformational states have been observed.

Table 7. Structural differences among several cytochrome c's

	6th ligand side	5th ligand side
horse oxidized[29]	open	open
bonito oxidized*	closed	open
bonito reduced	closed	open
tuna reduced[47]	closed	closed

* The protein was oxidized in crystalline state.

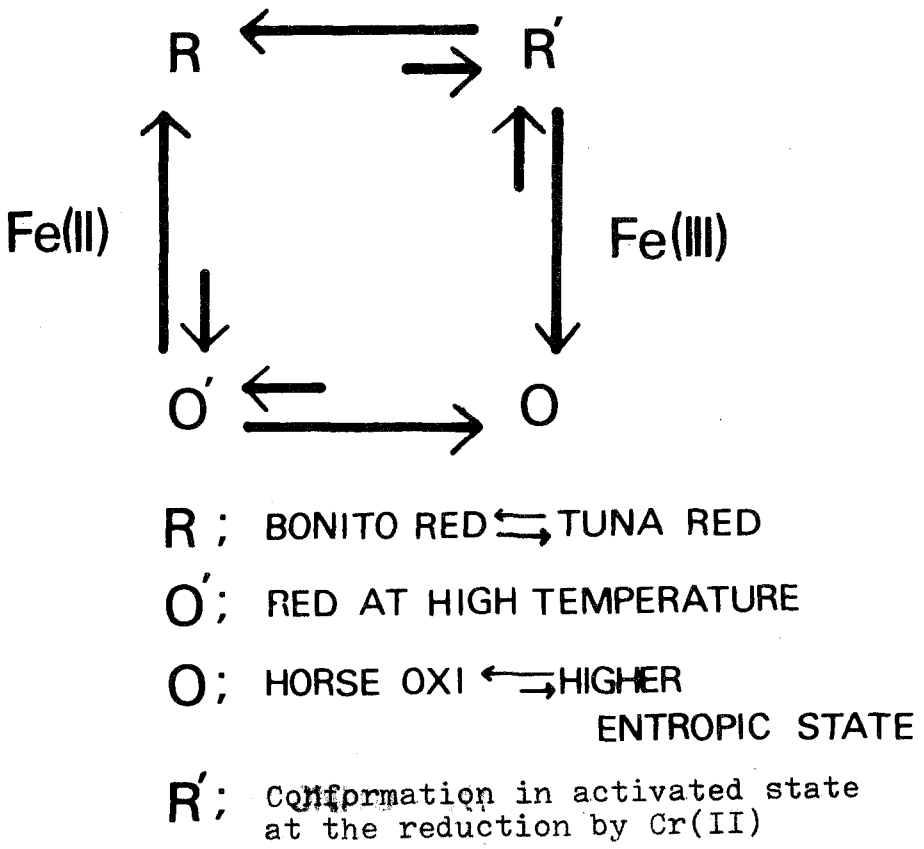

Fig. 23. Cyclic oxidation and reduction. The conformational states in "R" and "O" are the reduced and the oxidized, respectively, and the electronic states are also the reduced and the oxidized, respectively. The conformations of "R'" and "O'" are similar to the reduced and the oxidized, and the electronic states are the oxidized and the reduced, respectively.

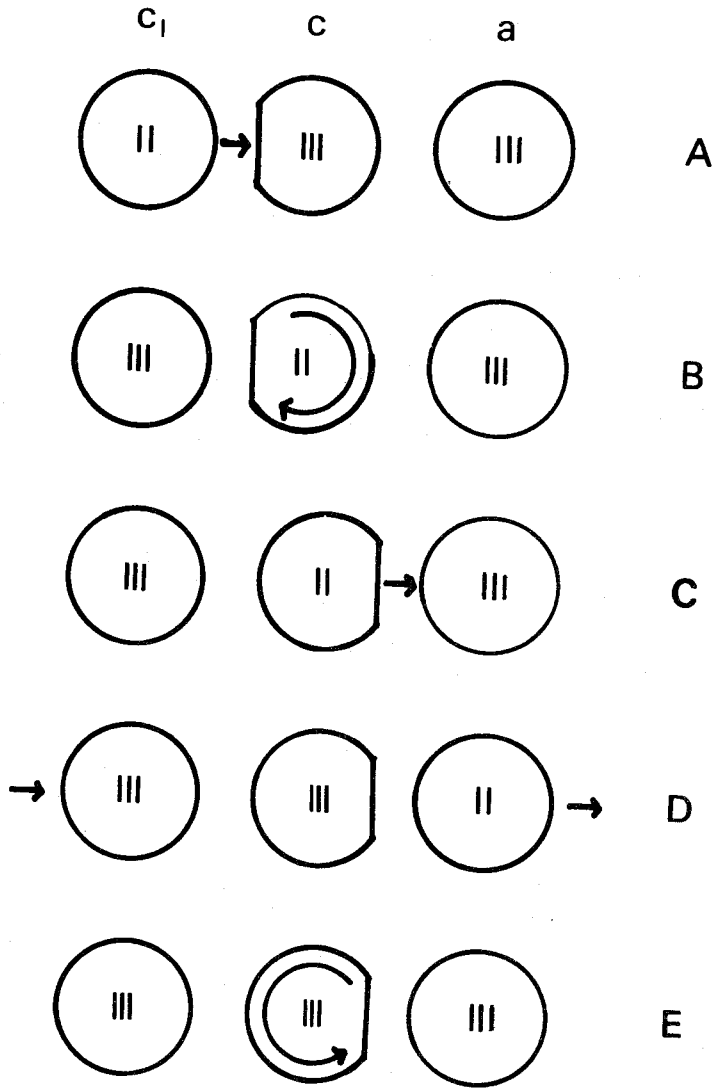

Fig. 24. Schematic diagram indicating electron transfer between adjacent cytochromes and rotation of cytochrome c, according to Chance et al.[40] "II" and "III" represent the heme iron to be in ferrous and ferric states, respectively.

A: An electron is transferred from cytochromes c_1 to c.

B; Rotation of cytochrome c occurs.

C: An electron is transferred from cytochromes c to a.

D: Cytochrome c_1 accepts an electron and a removes one.

E: Cytochrome c rotates and becomes in the same state as A.

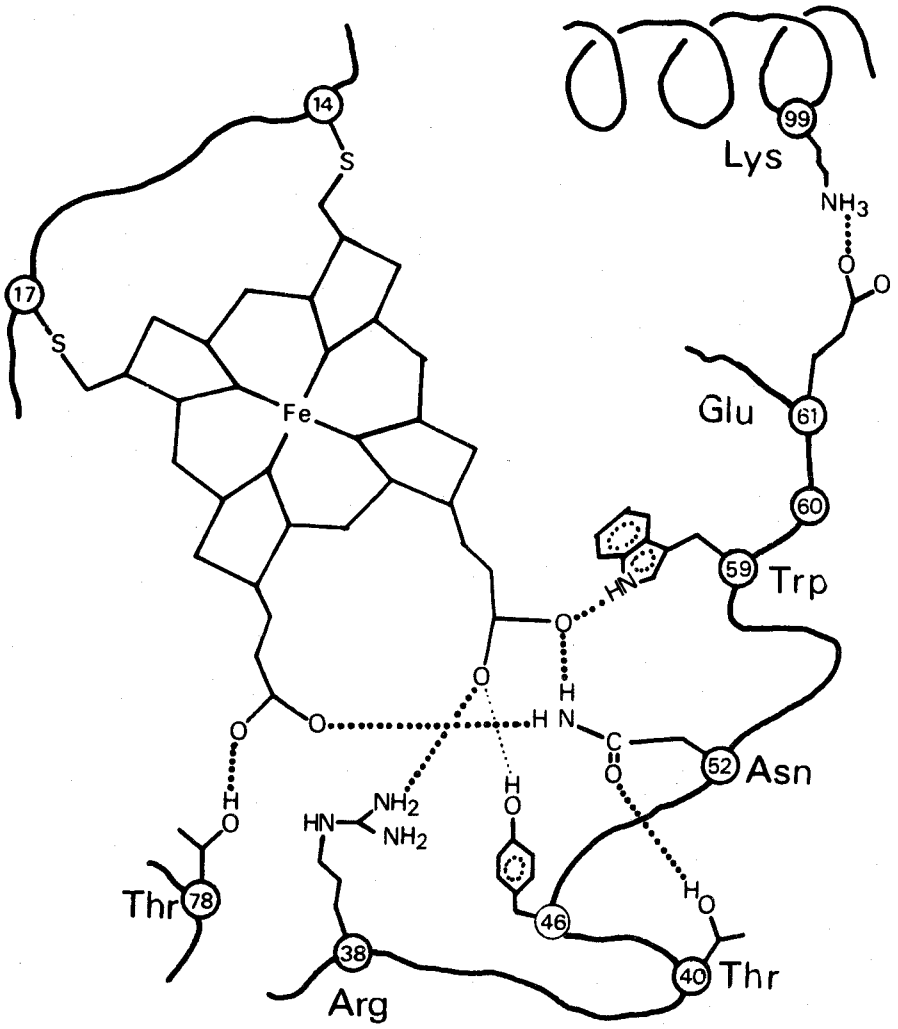

Fig. 25. Network of hydrogen bonds in the lower part of the bonito ferrocytochrome c. Dotted lines show hydrogen bonds, and heavy dotted ones represent the bonds between conservative residues. Heavy circles show the conservative residues. Tertiary structure of the protein seems to be kept by these specific hydrogen bonds.

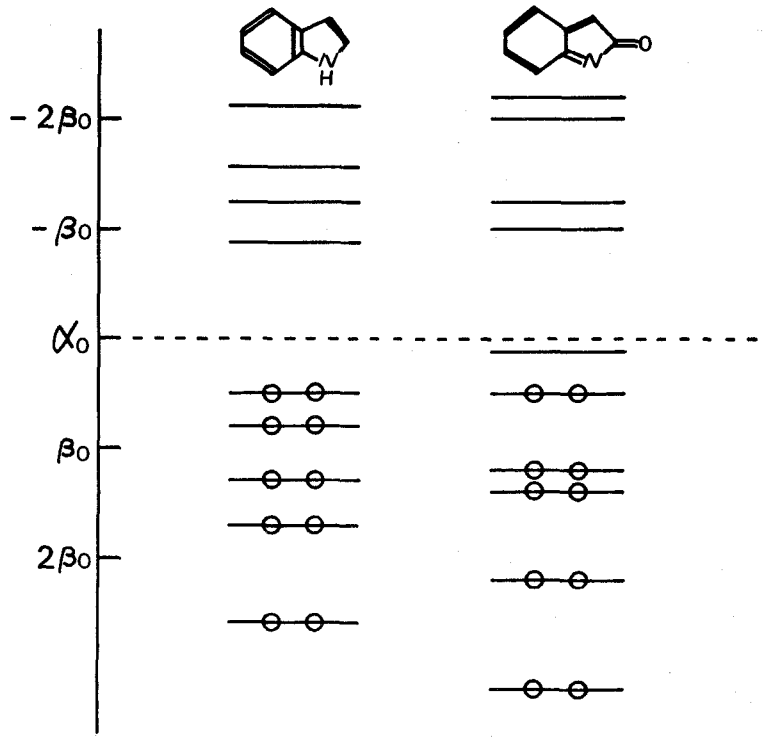

Fig. 26. The diagrams of π-electron energy level for the indole and the oxidized indole systems. The calculations were carried out by a simple Hückel method using the parameters proposed by Ladik.[46] Open circles represent electrons in the ground states. The energy level of the lowest unoccupied orbital in the oxidized indole ring is lower than that in the unmodified ring.

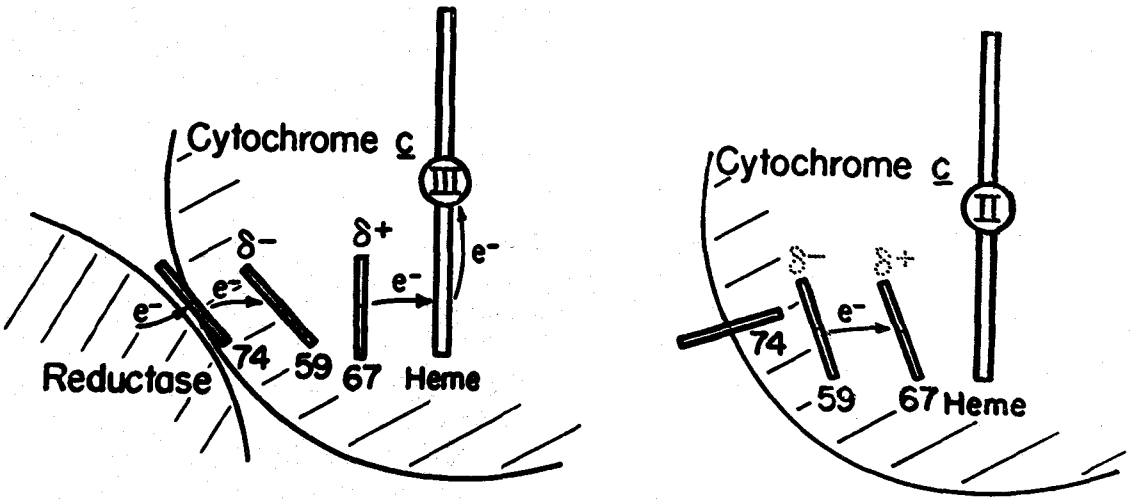

Fig. 27. One of the possible electron pathways proposed by Takano et al.[47] for the reduction of the iron atom. An electron from the reductase is transferred to the heme of cytochrome c through the aromatic rings of Tyr(74), Trp(59) and Tyr(67).

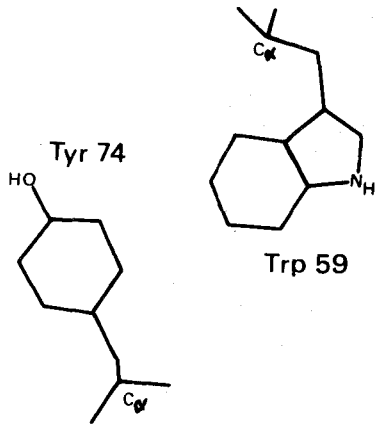

Fig. 28. Location of the aromatic groups of Tyr(74) and Trp(59) in the horse oxidized protein.[48] The rotation about C_α-C_β bond of Tyr(74) is necessary for the overlapping of the π-electron clouds of the groups.

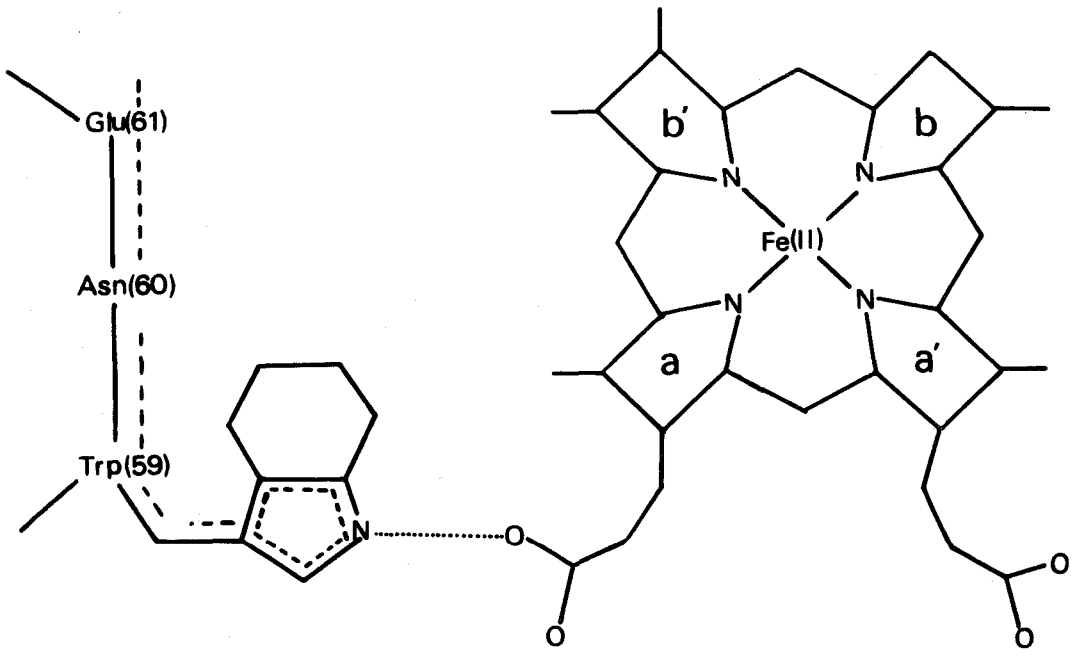

Fig. 29. One of the possible electron pathways from the molecular surface to Trp(59) for the reduction of the heme iron atom. The way of Glu(61)→ Asn(60)→ Trp(59) which has a rather extended conformation is the shortest pathway of the electron along peptide. An electron accepted at Glu(61) is trapped in the indole ring, and the electron may be transported to the heme directly or indirectly.

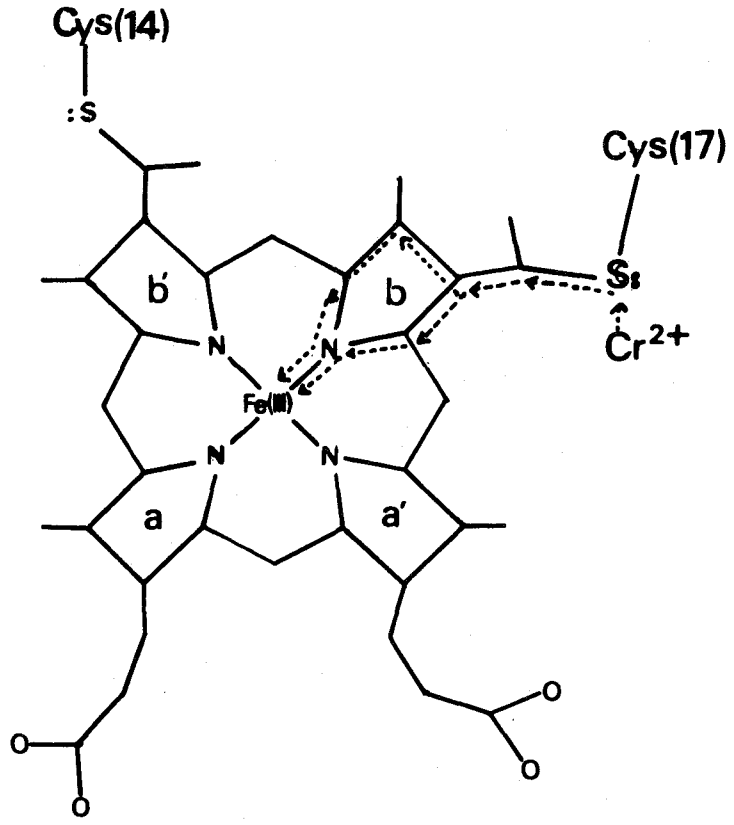

Fig. 30. An electron pathway for the reduction of the heme iron atom with chromous ion. The chromous ion is considered to react with a sulfur atom of Cys(17) which is exposed to the molecular surface. An electron donated on the sulfur is transferred to the iron through a pyrrole ring.

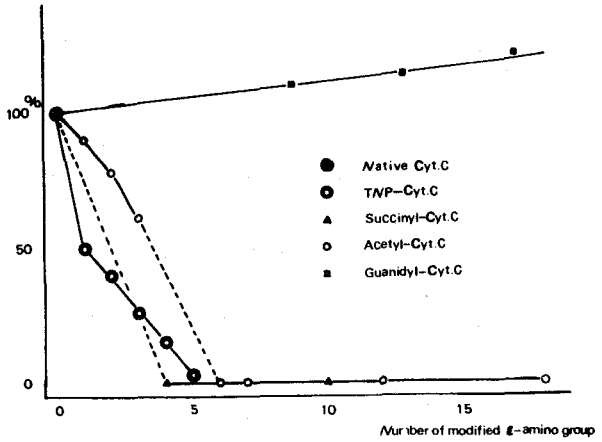

Fig. 31. The oxidase activity change by several chemical modification of lysyl groups.[51]

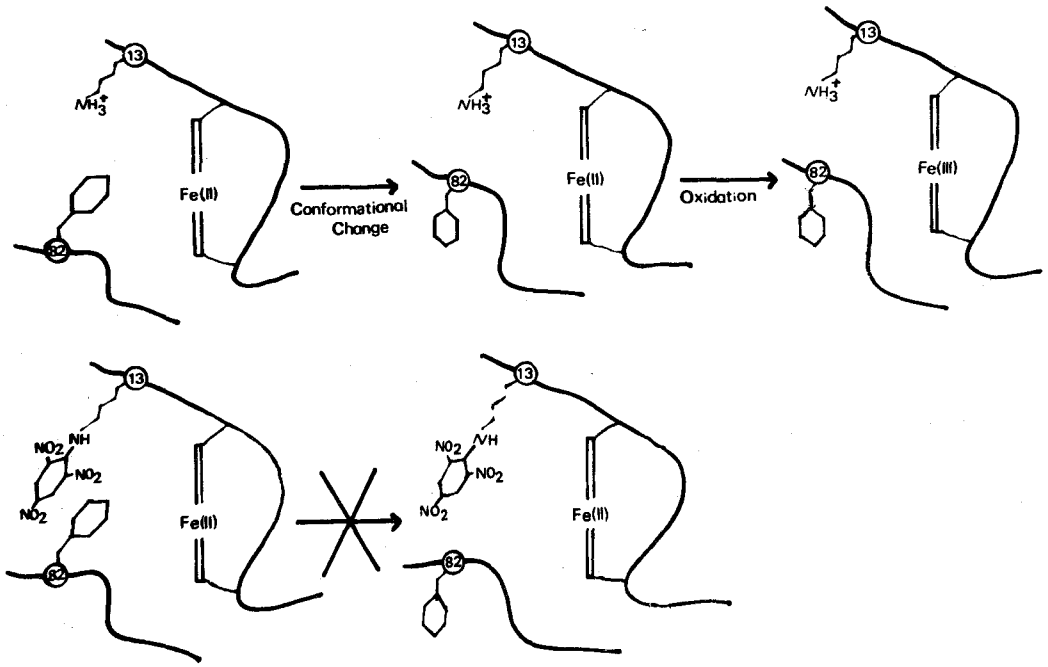

Fig. 32. Top, one of the possible oxidation scheme of cytochrome c. The conformational change of the protein is followed by the oxidation of the heme iron. In the first step, the phenyl ring of Phe(82) is converted from the inside of the molecule to the outside. In the second step, the heme iron is oxidized. Bottom, an assumed conformation of the modified cytochrome c whose Lys(13) is trinitrophenylated. The trinitrophenyl group of the modified protein may interact with the phenyl ring of Phe(82) in the reduced state. The interaction seems to make the conformational change difficult, so that the first step of the above oxidation scheme is disturbed. It may be one of the reason for the decrease of the oxidase activity of the protein by the modification.

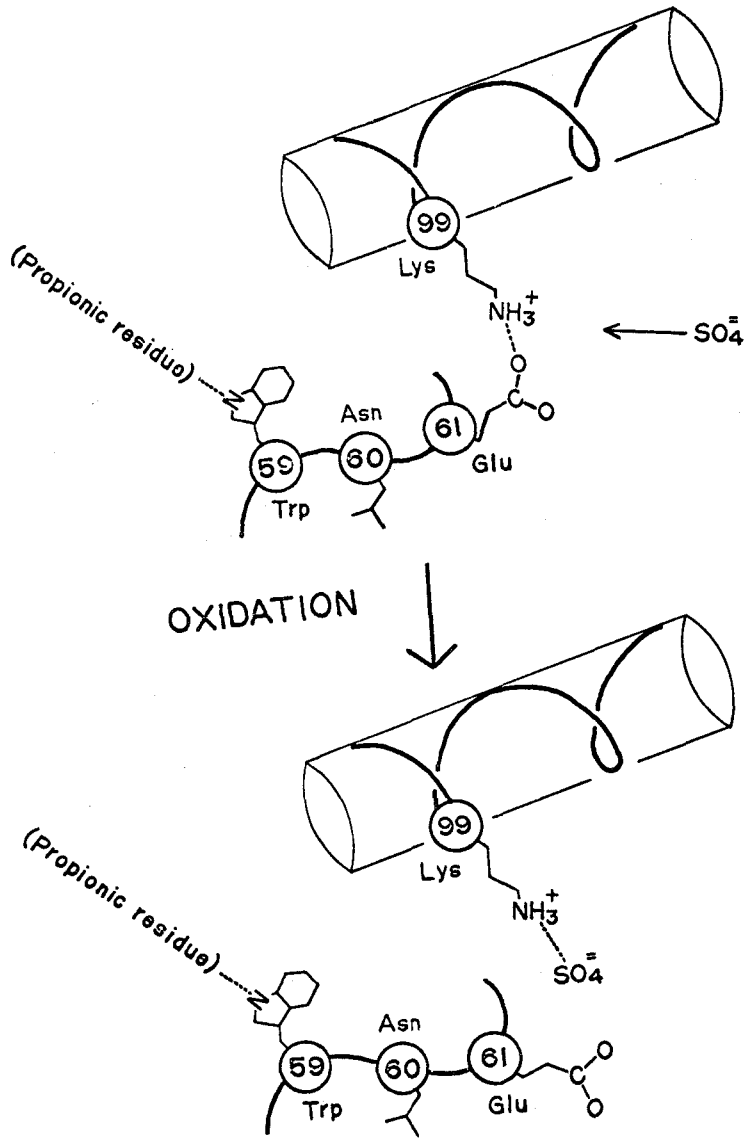

Fig. 33. Structure change upon oxidation and anion catching scheme of the protein. In the reduced state the amino group of Lys(99) is bound to carboxyl group of Lys(99) through a hydrogen bond. The binding between two groups is broken by the movement of main chain 59 through 62 upon oxidation of the iron atom, and then the amino group catches a sulfate anion.

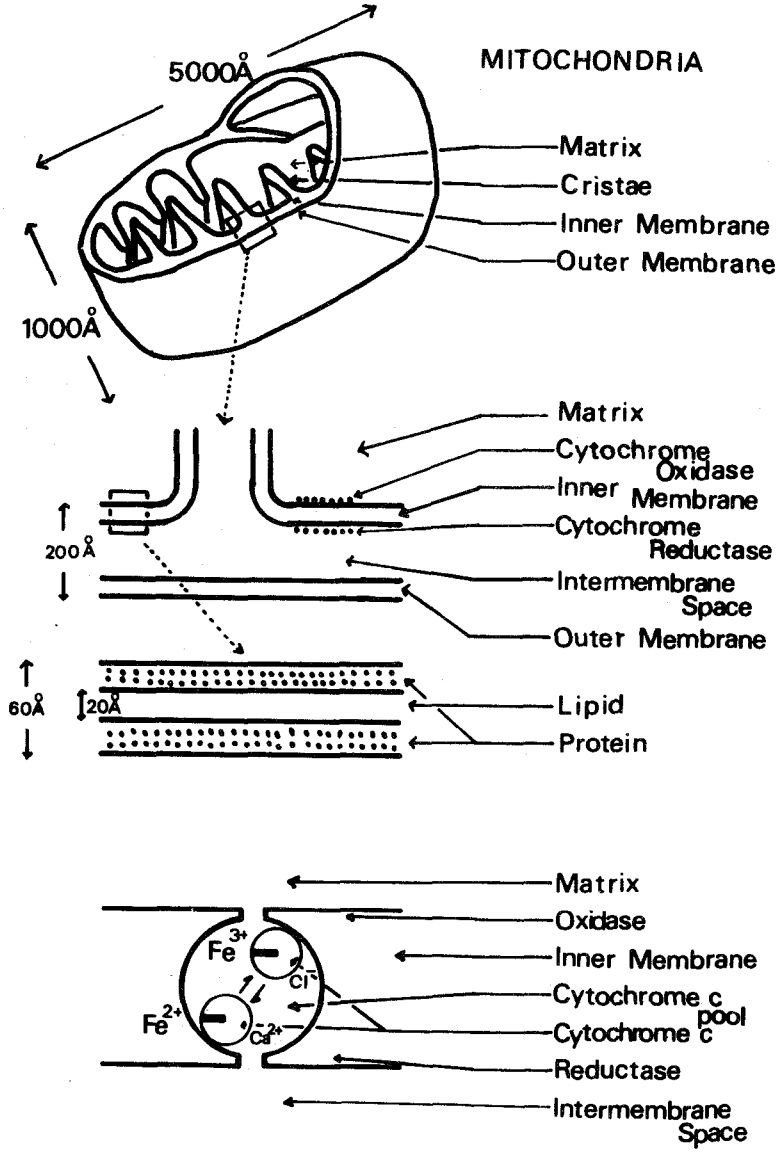

Fig. 34. A diagram of the ultra-structure of a mitochondria and ion-transport scheme of cytochrome c in the mitochondrial inner membrane. Top, three dimensional diagram which shows whole structure of a mitochondria, cristae, inner membrane and outer membrane. Bottom, the smaller circles in the cytochrome c pool represent the reduced cytochrome c (lower circle) and the oxidized (upper circle). The short heavy lines represnt the heme groups of the protein.

References

1) C.A.MacMunn, Proc. Roy. Soc. London, 39, 248(1886)

2) D.Keilin, ibid., 98B, 312(1925)

3) E.Margoliash and E.L.Smith, Nature, 192, 1121(1961)

4) G.Kreil and H.Tuppy, Nature, 192, 1123(1961)

5) R.E.Dickerson, Scientific American, 58, April(1972)

6) D.Keilin and E.C.Slater, Brit. Med. Bull., 9_, 89(1953)

7) T.Nakayama, K.Titani and K.Narita, private communucation

8) K.Zeile and F.Reuter, Z.Physiol. Chem., 221, 101(1933)

9) J.H.P.Jonxis, Biochem. J., 33, 1743(1939)

10) E.Stellwagen, Biochem., 3, 919(1964)

11) T.Yamanaka, H.Mizushima, M.Nozaki, T.Horio and K.Okunuki, J.Biochem., 405(1971)

12) A.G.Redfield and R.K.Gupta, Symp. Quantitative Biology, Vol.XXXVI, 405(1971)

13) P.Mcdermott, L.May and J.Orlando, Biophys.J., 615(1967)

14) T.Flatmark and A.B.Robinson, Structure and Function of Cytochromes, p.318(1968)

15) Y.P.Myer, Biochem., 7, 765(1968)

16) D.D.Ulmer, ibid., 4, 121(1959)

17) K.Ando, H.Matsubara and K.Okunuki, Biochem. Biophys. Acta, 118, 256(1966)

18) D.W.Butt and D.Keilin, Proc. Roy. Soc. London, B156, 429(1962)

19) D.D.Ulmer and J.R.Kagi, Biochem., 7, 2710(1968)

20) P.George and A.Schejter, J.Biol. Chem., 239, 1504(1964)

21) E.Margoliash, G.H.Barlow and V.BYERS, Nature, 228, 723 (1970)

22) I.Sekuzu, S.Takemori, Y.Orii, and K.Okunuki, Biochem. Biophys. Acta, 37, 64(1960)

23) E.Margoliash and O.F.Walasek, Method in Enzymology, Vol.10, p.339(1966)

24) H.W.Wyckoff, M.Doscher, D.Tsernoglou, T.Inagami, L.N.Johnson, K.D.Hardman, N.M.Allewell, D.M.Kelly and F.M.Richards, J.Mol.Biol., 27, 563(1967)

25) T.C.Furnas, Single Crystal Orienter Instruction Manual, Milwaukee, General Electric Company, (1956)

26) K.G.Paul, Acta Chem. Scand., 4, 239(1950)

27) D.M.Blow and F.H.Crick, Acta Cryst., 12, 794(1959)

28) R.E.Dickerson, J.C.Kendrew and B.E.Strandberg, Acta Cryst., 14, 1188(1961)

29) R.E.Dickerson, T.Takano, D.Eisenberg, O.B.Kallai, L.Samson, A.Cooper and E.Margoliash, J. Biol. Chem., 246, 1511(1971)

30) T.Takano, R.Swanson, O.B.Kallai and R.E.Dickerson, Symp. Quantitative Biology, Vol.XXXVI, 397(1971)

31) R.E.Dickerson, T.Takano and O.B.Kallai, Fifth Jerusalem Symposium, April(1972)

32) G.Kartha, Acta Cryst., 14, 680(1961)

33) D.M.Blow and M.G.Rossman, Acta Cryst., 14, 1195(1961)

34) A.Schejter and P.George, Biochem., 3, 1045(1964)

35) J.W.Dawson, H.B.Gray, R.A.Holwerda and E.W.Westhead, Proc. Nat. Acad. Sci. USA, 69, 30(1972)

36) B.Chance, In Heamatine Enzymes, ed. by J.E.Falk, R.Lemberg, and R.K.Morton, p.17, Oxford Pergamon Press, (1961)

37) Eherenberg and Theorell, Acta Chem. Scan., 9 1193(1955)

38) R.E.Dickerson, In Structure and Function of Cytochromes, ed. by Okunuki, M.D.Kamen, and I.Sekuzu, p.225, Tokyo University Press, (1968)

39) T.Ashida, T.Ueki, T.Tsukihara, A.Sugihara, T.Takano, and M.Kakudo, J. Biochem., 70, 913(1971)

40) B.Chance and G.R.Williams, Adv. Enzymol., 17, 86(1956)

41) K.Okunuki, In Oxygenases, ed. by Hayaish, p.449. New York; Academic Press, (1962)

42) Y.P.Myer, Biochem., 11, 4195(1972)

43) Y.P.Myer, ibid., 11, 4209(1972)

44) L.Smith, H.C.Davis, M.Reichin, and E.Margoliash, J.Biol. Chem., 248, 237(1973)

45) F.R.Salame, S.T.Freer, N.G.Xoung, R.A.Alden, and J.Kraut, private communication

46) T.A.Hoffman and J.Ladik, Adv. Chem. Phys., 7 84(1964)

47) T.Takano, O.B.Kallai, R.Swanson, and R.E.Dickerson, J. Biol. Chem., in press.

48) T.Takano, private communication

49) K.D.Kopple, R.R.Miller, and T.C.Muller, In Oxidase and Related Redox Systems, ed. by T.E.King, H.S.Mason, and M.Morrison, p.259, New York: John Wiley and Sons, (1964)

50) A.Kowalsky, J.Biol.Chem., 244, 6619(1969)

51) K.Wada and K.Okunuki, J. Biochem., 64, 667(1969)

52) S.Takemori et al, Nature, 195, 456(1962)

53) S.Takemori et al, J. Biochem., 52, 28(1962)

54) N.Kitahara, A.Endo, H.Mizushima, and H.Okazaki, Seikagaku, 39, 161(1967)

55) P.Nicholls, Arch. Biochem. Biophys., 106, 25(1964).

56) Y.Orii, I.Sekuzu, and K.Okunuki, J.Biochem., 51, 204 (1962).

57) F.C.Young, and T.E.King, Biochem. Biophys. Res. Commun., 47, 380(1972).

58) A.Fonyo, Biochem. Biophys. Res. Commun., 32, 624(1968).

59) D.D.Tyler, Biochem. J., 111, 665(1969).

60) A.J.Meijer, G.S.P.Groot, and J.M.Tager, FEBS Letters, 8, 41(1970).

List of Publications

I. The present thesis has been published in the following papers.

1. The Crystal Structure of Bonito (Katsuo) Ferrocytochrome c at 4Å Resolution.
   T.Ashida, T.Ueki, T.Tsukihara, A.Sugihara, T.Takano, and M.Kakudo, J. Biochem., 70, 913-924 (1971).

2. The Crystal Structure of Bonito (Katsuo) Ferrocytochrome c at 2.3Å Resolution.
   T.Ashida, N.Tanaka, T.Yamane, T.Tsukihara, and M.Kakudo, J. Biochem., 73, 463-465 (1973).

3. Oxidation of a Ferrocytochrome c in the Crystalline State —— Structural Change and Anion Binding.
   T.Tsukihara, T.Yamane, N.Tanaka, T.Ashida, and M.Kakudo, J. Biochem., 73, 1163-1167 (1973).

II. List of the related papers.

1. The Crystal Structure of Two Forms of 1-Ethyl-5-bromouracil.
   H.Mizuno, N.Nakanishi, T.Fujiwara, K.Tomita, T.Tsukihara, T.Ashida, and M.Kakudo, Biochem. Biophys. Res. Comm., 41, 1161-1165 (1970).

2. The Crystal Structure of 1-Ethyl-5-bromouracil. II. The Crystal Structure of the Form II Crystal of 1-Ethyl-5-bromouracil.
   T.Tsukihara, T.Ashida, and M.Kakudo, 45, 909-912 (1972).

3. The Crystal Structure of L-Citrulline Hydrochloride and L-Homocitrulline Hydrochloride.
T.Ashida, K.Funakoshi, T.Tsukihara, T.Ueki, and M.Kakudo, B 28, 1367-1374 (1972).

4. The Crystal Structure of o-Nitrobenzamide.
K.Fujimori, T.Tsukihara, Y.Katsube, and J.Yamamoto, Bull. Chem. Soc. Japan, 45, 1564-1565 (1972).

5. The Crystal and Molecular Structure of Bis(L-prolinamidato)-nickel(II) Dihydrate.
T.Tsukihara, Y.Katsube, K.Fujimori, and Y.Ishimura, Bull. Chem. Soc. Japan, 45, 1367-1371 (1972).

6. The Crystal and Molecular Structure of Averufin.
Y.Katsube, T.Tsukihara, N.Tanaka, K.Ando, T.Hamasaki, and Y.Hatsuda, Bull. Chem. Soc. Japan, 45, 2091-2096 (1972).

7. The Crystal Structure of Cupric Complex with Succinimide. I. Cesium Tetrakis(succinimidato)copper(II) Dihydrate.
T.Tsukihara, Y.Katsube, K.Fujimori, and T.Ito, Bull. Chem. Soc. Japan, 45, 2959-2963 (1972).

8. Structure and Absolute Configuration of $(+)_{546}$-cis(O)-(Sarcosinate-N-monopropionato)triamminecobalt(III) Ion.
K.Okamoto, T.Tsukihara, J.Hidaka, and Y.Shimura, Chemistry Letters, 145-148 (1973).